Characterisation of single tryptophan mutants of Saccharomyces cerevisiae Ire1

JANICKAITE, DONATA

Abstract

The endoplasmic reticulum (ER) is responsible for the folding and modifications of numerous proteins produced by the cell. To ensure that only correctly folded proteins proceed to the surface, a highly conserved process called the unfolded protein response (UPR) has been developed. In mammals, signalling in the UPR is induced by membrane embedded stress sensors, IRE1, PERK and ATF6. IRE1 is the only ER stress sensor conserved across all eukaryotes.

Yeast Ire1 has a serine/threonine kinase and endoribonuclease domains needed to exert its functions. During accumulation of unfolded or misfolded proteins, Ire1 oligomerises and autophosphorylates leading to the activation of its RNase domain. The activated RNase domain then targets mRNA to remove an intron and produce a bZIP transcriptional activator (Hac 1 in yeast and XBP-1 in metazoans), which activates the downstream pathways of UPR. The aim of this study was to purify and characterise the enzymatic activity of tryptophan mutants of yeast Ire1 in order to potentially use them in future tryptophan fluorescence studies.

Three single tryptophan mutants were purified as GST-fusion proteins and characterised for kinase and RNase activity. Results presented in this thesis show one of the mutants (W855F-W1025F-Ire1) purifies well based on previously optimised protocols and two mutants probably purify as a mixture of full length and truncated proteins. All of the tryptophan mutants retain kinase activity, but only one of them has partial RNase activity (W855F-W981F-Ire1). It is also shown here that removal of the GST tag decreases the protein RNase activity, potentially because the protein becomes monomeric.

Further optimisation of the induction and purification conditions is needed to obtain full length proteins. Alternatively, it may be necessary to use a different induction system for protein purification.

CHARACTERISATION OF SINGLE TRYPTOPHAN MUTANTS OF *SACCHAROMYCES CEREVISIAE* Ire1

Donata Janickaite

This thesis is submitted for the degree of Master of Science by Research (MScR)

School of Biological and Biomedical Sciences

Durham University

December 2016

Contents

List of abbreviations

1NM-PP1	1-(1,1-dimethylethyl)-3-(1-naphthalenylmethyl)-1*H*-pyrazolo[3,4-d]pyrimidin-4-amine
ADP	adenosine diphosphate
APS	ammonium persulfate
ATF6	activating transcription factor 6
ATP	adenosine triphosphate
BiP	binding immunoglobulin protein
BSA	bovine serum albumin
bZIP	basic leucine zipper
DEPC	diethyl pyrocarbonate
DNA	deoxyribonucleic acid
EDTA	ethylenediaminetetraacetic acid
ER	endoplasmic reticulum
ERAD	endoplasmic reticulum-associated degradation
Gly	glycine
GRP78	78 kDa glucose-regulated protein
GRP94	94 kDa glucose-regulated protein
GST	glutathione *S*-transferase
Hac1	homologous to Atf/Creb1
HEPES	4-(2-hydroxyethyl)-1-piperazineethanesulfonic acid
Hsp70	heat shock protein of 70 kDa
Hsp90	heat shock protein of 90 kDa
Ire1	inositol requiring 1
LB	Lysogenic broth
mRNA	messenger RNA
PAGE	polyacrylamide gel electrophoresis
PBS	phosphate-buffered saline
PERK	pancreatic ER eIF2α kinase
Phe	phenylalanine
PMSF	phenylmethanesulphonyl fluoride
RNA	ribonucleic acid
S1P	site-1 protease
S2P	site-2 protease
SDS	sodium dodecyl sulphate
TAE	tris/acetate/EDTA
TBE	tris/borate/EDTA
TE	tris/EDTA
TEMED	*N*,*N*,*N*',*N*'-tetramethylethylenediamine
TM	transmembrane
Tris	tris(hydroxymethyl) methylamine
tRNA	transfer RNA
Trp	tryptophan
UPR	unfolded protein response
WT	wild type
XBP-1	X-box binding protein 1

List of figures

List of tables

Statement of Copyright

Acknowledgements

Wow, what a journey! I cannot believe it’s nearly over!

First of all, I would like to express my sincere gratitude to Dr Martin Schröder for giving me the opportunity to join his lab and have one of the most exciting years of my life. Thanks for all the patience and support during this project, your commitment to science is really inspiring. It has been an invaluable experience for my career, and hopefully, I have also grown as a person, at least a little bit.

Thanks to everyone who worked in the lab with me, no matter if it was the whole year, or just a few weeks, people in lab 2 have always been the best. Thanks to Max Mushens-Brown for spending his precious time in the cold lab and helping me with chromatography. Thanks to Joey Nelson for all the hugs and for the hotline bling (cannot believe I actually wrote that). A huge thank you to Maha Al-rushadi for all the amazing time in the lab and in the real world! A very special thanks to Mike Armstrong for motivating me to keep the lab bench tidy, for the music, for showing me the wonders of Yorkshire, for the best company during the weekends and for countless other things! Most importantly, thank you for submitting this thesis! To all the other lovely people in the department, you made this year absolutely incredible. Thank you!

I am also thankful to my family and friends for all the love and support. Thanks for keeping me company during the long incubation and protein purification steps and also for coming to Durham to visit me. I am incredibly lucky to have so many wonderful people around.

Lastly, I would like to thank my parents for the financial support. It would not have been possible without you.

Dedicated to the memory of Eugenijus Eimutis Redkus

1 Introduction

The healthy existence of any organism is dependent on reliable cell signalling. Signals must be received and interpreted correctly for normal cell development, immune response, tissue homeostasis, etc. Faulty signalling often leads to a variety of diseases including cancer (Clarke et al., 2014), autoimmunity (Todd et al., 2008), and diabetes (Özcan et al., 2004). Much information required for this process is transmitted by either secreted or membrane - embedded proteins. All these proteins in eukaryotic cells enter the secretory pathway to be folded and modified in the endoplasmic reticulum (ER). The process of folding can be impaired by a variety of physiological or metabolic conditions that threaten cell survival such as extreme temperature changes, toxins, and viral infections (Lee, 1992) leading to accumulation of misfolded proteins, which activates the unfolded protein response (UPR). Only correctly folded proteins are allowed to move along the secretory pathway towards the Golgi apparatus. Therefore, the UPR has three main aims: reduce global mRNA translation, activate the molecular chaperones that increase the ER folding capacity and stimulate ER-associated degradation (ERAD) of misfolded proteins (Cao and Kaufman, 2012). However, if the UPR cannot deal with the amount of unfolded or misfolded proteins using the three main strategies – programmed cell death or apoptosis will be activated (Fribley et al., 2009).

1.1 The Unfolded Protein Response

The ER is a membrane enclosed compartment responsible for protein folding, storage and transportation. It is the first step of the secretory pathway. Proteins enter the ER as nascent polypeptide chains during translation where they undergo folding and post-translational modifications. The key proteins responsible for folding in the ER are foldases and chaperones. Some proteins stay in the ER, but most move along the secretory pathway and become distributed throughout the organelles and different membranes.

The UPR is a highly conserved process found in mammalian, plant, yeast, fly and worm cells (Mori, 2009) which evolved to ensure correct protein folding and normal ER function. An ER stress signal arising from its lumen is transmitted across the membrane by transmembrane (TM) proteins. In mammalian cells, three TM proteins are involved in transmitting UPR signals: inositol-requiring 1 (IRE1), pancreatic ER eIF2α kinase (PERK), and activating transcription factor 6 (ATF6). Interestingly, the complexity of UPR increases with evolution from only one functional TM protein in *Saccharomyces cerevisiae* (Ire1), two in *Caenorhabditis elegans* and *Drosophila melanogaster* (ire-1 and pek-1), and three in mammals (IRE1, PERK and ATF6) (Mori, 2009).

A prototype of UPR was first mentioned in the literature in 1977, when virus-transformed chick embryo fibroblasts had increased levels of novel proteins GRP78 and GRP94 in the absence of glucose (Shiu et al., 1977). The synthesis of the two glucose-regulated proteins was later shown to be induced by accumulation of unfolded proteins by other stress factors including treatment with glycosylation inhibiting drugs, calcium ionophores or amino acid analogues (Kozutsumi et al., 1988). GRP78 was also reported to have a sequence similar to the sequence of a heat shock protein, Hsp70 (Munro and Pelham, 1986), and to be identical to an Ig heavy chain-binding protein BiP (Hendershot et al., 1988), which binds to misfolded proteins that accumulate in the ER. GRP94 was found to belong to the Hsp90 family of ER molecular chaperones. These findings suggested that both proteins were involved in maintaining the homeostasis in the ER by neutralising and removing the accumulated misfolded proteins. GRP78/BiP was initially believed to play a key role in

the UPR, because of its capacity to bind to all three ER stress transducers in mammalian cells and to keep them in an inactive state (Figure 1.1). In conditions of ER stress, BiP is released from the UPR regulators and binds to unfolded or misfolded proteins leading to the activation of the UPR regulators and downstream signaling molecules. IRE1 and PERK homodimerise through their lumenal domains, autophosphorylate and become activated (Bertolotti et al., 2000). ATF6 is cleaved by site-1 protease (S1P) and site-2 protease (S2P) to release its cytosolic domain, which travels to the nucleus, where it acts as a transcription factor for UPR target genes including GRP78 and GRP94 (Ye et al., 2000). However, BiP is essential for protein folding and translocation in the ER, therefore, mutants of BiP cause ER stress and it is hard to determine whether activation of Ire1 is a result of the mutations in BiP or a result of different ER conditions (Gardner et al., 2013). In 2004, it was shown that the lumenal domain of Ire1 has two regions essential for activity and BiP-binding sites do not belong to any of them. It was also shown that deletion of the BiP-binding site stopped BiP from binding to UPR signal transducing proteins. However, Ire1 remained inactive in the absence of ER stress. Therefore, it was concluded that BiP could not be the principal factor determining Ire1 activity (Kimata et al., 2004).

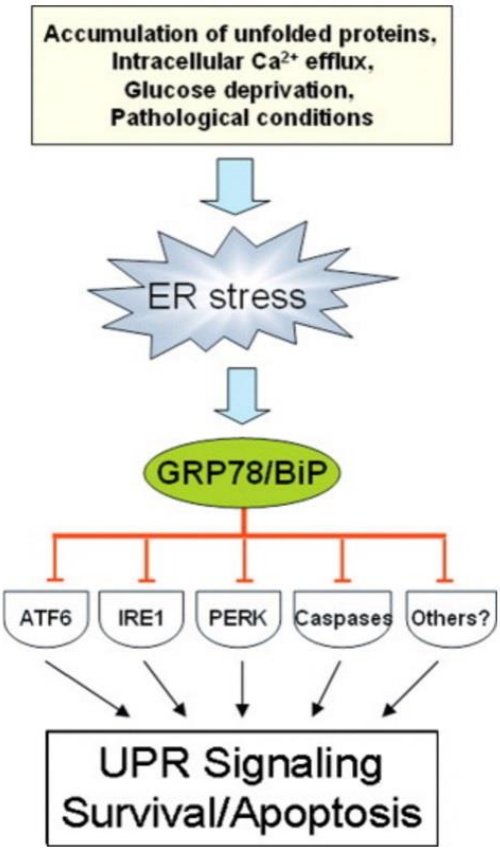

Figure 1.1. An early ER stress model.
A model of ER stress suggesting that BiP is the central player responsible for activating UPR signaling. (Lee, 2005)

1.2 The structure and function of Ire1

Ire1 is the only ER stress sensor conserved across all eukaryotes. It is a regulatory protein that alters gene expression as a result of endoplasmic reticulum stress. Ire1 is composed of five major functional domains (Figure 1.2). Two homologues of Ire1 are present in mammalian cells: Ire1α and Ire1β. Ire1α is universally expressed, while Ire1β expression is restricted to intestinal epithelial cells (Bertolotti et al., 2001). The N-terminal lumenal domain senses stress and transmits a signal across the membrane leading to dimerisation of Ire1 (Shamu and Walter, 1996). Oligomerisation leads to autophosphorylation by its cytoplasmic serine/threonine kinase domain and phosphorylation of downstream molecules in the UPR pathway.

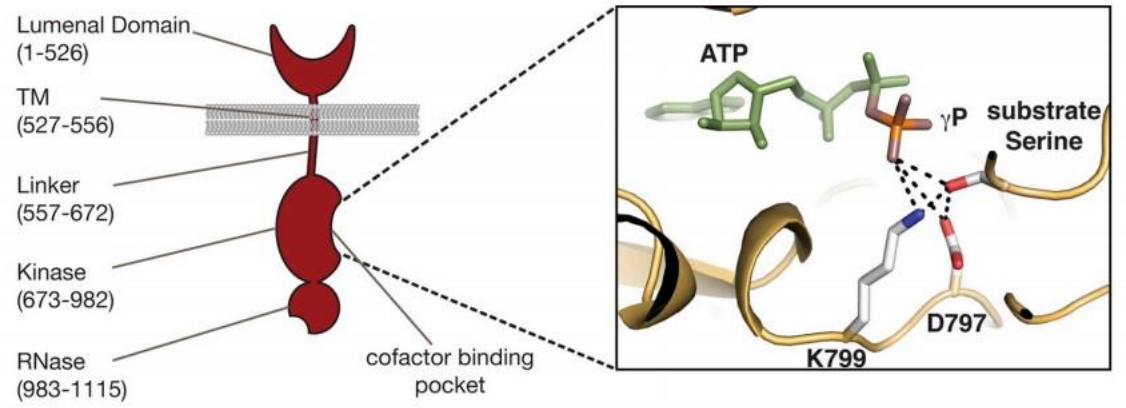

Figure 1.2. Schematic representation of the structure of Ire1.
On the left, a schematic representation of the structure of yeast Ire1 showing the five functional domains and the boundaries of each in terms of amino acid sequence. On the right, a model proposed by (Rubio et al., 2011), suggesting that conserved D797 and K799 in the nucleotide binding pocket catalyse phosphate transfer to substrate serine.

Studies show that mutations in the conserved K702 residue in the kinase domain of Ire1 prevent UPR activation (Mori et al., 1993) suggesting that the kinase activity is crucial for Ire1 to activate the unfolded protein response. Kinase autophosphorylation results in activation of the endoribonuclease (RNase) domain, which specifically cleaves precursor mRNAs (*HAC1* in *S. cerevisiae* and *Xbp1* in metazoans) to remove an intron and to generate a functional transcriptional activator. However, this process can be bypassed using ATP-competitive kinase inhibitors (see next paragraph). HAC1 exons in yeast are joint by a tRNA ligase Rlg1p (Sidrauski et al., 1996). Intron removal leads to a translational frame shift, which produces a potent basic leucine zipper (bZIP) transcription factor. The active transcription factor up-regulates UPR target genes and leads to increased folding capacity of the ER. The recently identified RtcB ligase joins the two XBP-1 exons in metazoans (Kosmaczewski et al., 2014; Lu et al., 2014).

1.3 Efficient Ire1 activity is dependent on cooperation of the kinase and endonuclease domains

The activity of Ire1 is highly cooperative and full RNase activity is only obtained upon oligomerisation of various Ire1 molecules (Korennykh et al., 2009). The crystal structure reveals a symmetric back-to-back organisation of the kinase domains attached to an RNase dimer with two separate active sites (Lee et al., 2008). The crystal structures of human IRE1α also reveal that states of limited RNase activity are consistent with inactive kinase conformations while active endonuclease domains are consistent with active kinase conformations (Joshi et al., 2015). The formation of higher order oligomers is enabled by the active, nucleotide-bound conformation of the kinase. Initial studies supported the hypothesis that phosphorylation by the kinase domain is essential for activation of the RNase domain. However, in the presence of an ATP-competitive kinase inhibitor, 1NM-PP1, the UPR was retained suggesting that a conformational change rather than phosphorylation was key for Ire1 function (Papa et al., 2003). From this finding, it was further suggested that 1NM-PP1 must enforce a closed conformation and stimulate dimerisation and activation of the RNase domain (Lee et al., 2008). It was also suggested, that 1NM-PP1 binding may be so different from ADP binding that Ire1 becomes unresponsive to the phosphorylation status or that the binding is strong enough to shift the inhibitory conformation of the activation segment.

1.4 Understanding the Ire1 protein kinase activity by looking at the evolutionary conservation of other kinases

Phosphorylation is essential for a variety of cellular functions including protein regulation and signal transduction. Protein kinases are responsible for catalysing this reaction. One of the most common mechanisms for regulating the protein kinases is phosphorylation of the activation loop (Nolen et al., 2004). cAMP-dependent protein kinase (PKA) is one of the best studied protein kinases. It was actually the first kinase to have a solved crystal structure of the catalytic subunit (Knighton et al., 1991). The kinase was in an active conformation and showed that the activation loop has

nucleotide binding segment and a larger peptide binding segment. It was also shown that the amino acid residues in the catalytic core are conserved among other kinases. One of the older crystal structures in the unphosphorylated state (Zhang et al., 1994) shows that the domains of inactive ERK2 are more separated than PKA in the active conformation. Peptide binding is also inhibited by Y185 residue, which is phosphorylated in the active kinase. Other kinases adopted various different conformations (Goldberg et al., 1996; Hubbard et al., 1994), which explains the specificity for target ligands. The activation segment has been defined as the region between two conserved tripeptide motifs, DFG and APE. The sequence in between typically contains 20 – 35 residues. The DFG motif forms a Mg^{2+} binding site and the rest of the sequence forms a short β sheet β9, the activation loop, and the P+1 loop (Nolen et al., 2004). Comparison of the homology between the activation segments of different kinases showed conservation in both ends of the activation segment, but much less in the activation loop itself. This explains the diversity of the inactive kinase conformations and supports the specificity for different ligands.

Several mutations in the core cytosolic area affecting the Ire1 activity have been fairly well studied and understood. K702 found in the catalytic region is predicted to facilitate nucleophile attack by contacting the α- and β-phosphates and to neutralise the negative charges on the β-phosphate, which increase when the bond to the γ-phosphate of ATP is cleaved. K702 was reported to be essential for Ire1 activity (Mori et al., 1993). D828 is found within the conserved Asp–Phe–Gly (DFG) kinase motif and is predicted to coordinate β and γ phosphates of ATP with Mg^{2+}. D828A mutants have been proposed to bind ATP but not be able to autophosphorylate (Chawla et al., 2011). However, these data are not very reliable because it is unclear whether the authors corrected their data for binding of fluorescently-labelled nucleotides for inner filter effects. Therefore, their observation of D828A mutant binding ATP and further assumptions that nucleotide binding mimics an active RNase conformation required for mRNA splicing may be questionable. D797 and K799 were suggested to act as catalytic residues involved in coordinating the terminal ATP phosphate and catalysing phosphate transfer (Rubio et al., 2011) (Figure 1.2). In analogy to other protein kinases, the catalytic aspartate D797 is believed to bind the nucleophile and orient it for attack onto the γ-phosphate. The lysine two residues away (K799) is thought to

contact the γ-phosphate, neutralise negative charges and facilitate attack of the nucleophile (Endicott et al., 2012). Most of these mutants were reported to lack kinase or RNase activities (Chawla et al., 2011) and are therefore useful for studying the activity and structural characteristics of Ire1. The effect of the K799A mutation has not yet been described in the literature. Mutations in conserved endonuclease domain residues disrupted the RNase activity, but could autophosphorylate efficiently (Tirasophon et al., 2000) suggesting that RNase activity is not required for kinase activity.

The molecular mechanism of oligomerisation and RNase domain activation are not completely clear. It is generally agreed that the kinase domain is key for stress response, but different hypotheses have been suggested for how it may be inactivated (Sicheri and Silverman, 2011). One publication suggested that trans-autophosphorylation in the hyperphosphorylation loop (a highly phosphorylated 28-amino acid loop at residues 864 to 892) of Ire1 is required for disassembly and works as a reset mechanism (Rubio et al., 2011). Another paper argues that de-phosphorylation rather than phosphorylation is the switch for UPR attenuation (Chawla et al., 2011).

1.5 Using tryptophan mutants to observe conformational changes in Ire1

Extensive preliminary work in our laboratory suggests that K799, N802 and D828 are the key residues controlling the RNase activity (Schröder, unpubl.). A novel model for the control of RNase activity by the kinase domain has been proposed, but further evidence and appropriate controls are needed to support the hypothesis. We hypothesise that ATP-ADP hydrolysis cycles in the kinase domain are responsible for controlling RNase activity. The model suggests that ATP bound to the kinase domain inhibits RNase activity and ADP bound to the kinase domain activates the RNase domain. This would explain the requirement for kinase activity *in vivo,* the inactivity of kinase mutants (D797A) and the bypass of kinase activity by 1NM-PP1. 1NM-PP1 is smaller than ATP and may mimic ADP. This may also explain the phenotypes of the K799A, N802A and D828A mutants, which have previously shown increased RNase

activity when introduced into D797A, because the residues contact the γ-phosphate directly (K799) or indirectly (N802 and D828) via Mg^{2+} ions. We will be trying to get experimental evidence to support this hypothesis based on the analogy to other kinases.

The model predicts that there are at least two distinct conformations of the RNase domain when ATP or ADP are bound to the kinase domain. This project aims to provide evidence using the intrinsic fluorescent properties of tryptophan.

Tryptophan is a non-polar aromatic amino acid used extensively in fluorescence studies for its intrinsic properties such as anisotropy, lifetimes, excitation and emission spectra. All these properties can be measured using fluorescence spectrophotometers. Tryptophan works as an intrinsic probe for studying the structure, dynamics and function of various proteins (Szabo and Rayner, 1980). The tryptophan fluorescence is sensitive to the environment and it can be used to report changes in protein conformation and interactions with other molecules. The excitation maximum of tryptophan in solution is ~280 nm and the emission maximum is ~350 nm. A conformational change leads to different accessibility of tryptophan to the solvent, which results in different levels of quenching of tryptophan fluorescence. For instance, in hydrophobic environment the fluorescence gets blue-shifted (Möller and Denicola, 2002). Small proteins often have only one tryptophan, which makes it easy to interpret experimental data. However, in the case of larger proteins, the detected fluorescence is mostly a combination of the fluorescence of individual aromatic residues. Therefore, having more than one tryptophan residue in the protein makes it unlikely for the Trp fluorescence decay to be monoexponential and mutating the other residues is often necessary to use fluorescence spectroscopy measurements for research. Protein fluorescence is usually excited at 280 nm or longer wavelengths. The tryptophan emission lifetime is ~2.6 ns and the quantum yield ranges from zero to 0.35 (Eftink, 1991), which is useful for interpreting the protein structure based on changes in fluorescence.

673 LVVSEKILGYGSSGTVVFQGSFQGRPVAVKRMLIDFCDIALMEIKLLTES

723 DDHPNVIRYYCSETTDRFLYIALELCNLNLQDLVESKNVSDENLKLQKEY

773 NPISLLRQIASGVAHLHSLKIIHRDLKPQNILVSTSSRFTADQQTGAENL

823 RILISDFGLCKKLDSGQSSFRTNLNNPSGTSGWRAPELLEESNNLQCQVE

873 TEHSSSRHTVVSSDSFYDPFTKRRLTRSIDIFSMGCVFYYILSKGKHPFG

923 DKYSRESNIIRGIFSLDEMKCLHDRSLIAEATDLISQMIDHDPLKRPTAM

973 KVLRHPLFWPKSKKLEFLLKVSDRLEIENRDPPSALLMKFDAGSDFVIPS

1023 GDWTVKFDKTFMDNLERYRKYHSSKLMDLLRALRNKYHHFMDLPEDIAEL

1073 MGPVPDGFYDYFTKRFPNLLIGVYMIVKENLSDDQILREFLYS

Figure 1.3. The sequence of yeast Ire1 kinase and RNase domains.
The kinase domain is in red, the RNase domain is in purple. The important residues for this study are marked in bold

Yeast Ire1 has a total of eight Trp residues, three of them are in the cytosolic domain at the positions 855, 981 and 1025. Figure 1.3 shows the amino acid sequence of WT yeast Ire1 kinase and endonuclease domains, which are important for this study. The kinase domain is marked in red and the RNase domain in purple. Important residues including K799, N802, D828 and the three tryptophan residues in the cytosolic region are marked in bold. For all analysis of Ire1, we only purify the cytosolic region of the protein, therefore, only these three Trp residues are considered important. The Trp fluorescence decay is exponential and the lifetime is extracted by fitting exponential functions to the measured decay curves. We will be mutating two of the three residues in the sequence at one time, because retaining only one Trp residue may allow measuring the lifetime of the decay of fluorescence of this single tryptophan. The term single tryptophan mutants used in the text will refer to Ire1 containing only one Trp residue. The approach used here should ultimately lead to the development of a new model to study nucleotide binding to Ire1 and test the hypothesis that the conformation of the RNase domain is different depending on the nucleotide bound to the kinase domain.

1.6 Aims and hypothesis

The aim of this project was to purify and characterise the enzymatic activities of the tryptophan mutants of Ire1. This was achieved by addressing the following objectives:

1. Expression and purification of three single Trp mutants, namely W855F-W981F-Ire1, W855F-W1025F-Ire1 and W981F-W1025F-Ire1 as N-terminal GST-fusion proteins.
2. Measurement of the kinase activity of these mutants using *in vitro* kinase autophosphorylation assay. This will determine whether the protein kinase activity is affected by the mutations.
3. Measurement of the RNase activity of the mutants by *in vitro* XBP-1 splicing assay. This will determine if the mutants retain the RNase activity.
4. Cleavage of the GST tags using thrombin and further characterisation of the kinase and RNase domains because only those tryptophan mutants with RNase and kinase activities can be used as reliable models for studying the conformational changes using fluorescence spectroscopy.
5. Large scale purification and thrombin cleavage of the mutants, which retain both kinase and RNase activities.

2 Materials and Methods

2.1 Materials

The following chapter summarises all the materials used for the experiments in this study. Any specific preparation or storage instructions for the solutions are described in the notes section.

2.1.1 *Escherichia coli* strains

Table 1. List of *E. coli* strains used in this study

Name	Genotype	Source
BL21-CodonPlus (DE3)-RIL	*E. coli* B F$^-$ *ompT hsdS*(r_B^- m_B^-) *dcm*$^+$ Tet^r *gal* λ(DE3) *endA* Hte [*argU ileY leuW* Cam^r]	Agilent Technologies, Stockport, UK, cat. no. 230245
XL-10 GOLD	Tet^{r}Δ (*mcrA*)183 Δ(*mcrCB-hsdSMR-mrr*)173 *endA1 supE44 thi-1 recA1 gyrA96 relA1 lac* Hte [F´ *proAB lacI*^{q}*ZΔM15* Tn*10* (Tet^r) Amy Cam^r]	Agilent Technologies, Stockport, UK, cat. no. 200314

2.1.2 Plasmids

Table 2. List of plasmids used in this study

Name	Features	Source
pGEX-1λT-W855F-W981F- C'(S658)-IRE1	*P_{tac}-GST- W855F-W981F-C'IRE1 lacI bla*	Sergej Šesták, Slovak Academy of Sciences, Institute of Chemistry, Dubravska cesta 9, Bratislava 84538, Slovakia.
pGEX-1λT-W855F-W1025F- C'(S658)-IRE1	*P_{tac}-GST-W855F-W1025F-C'IRE1 lacI bla*	Sergej Šesták,
pGEX-1λT-W981F-W1025F- C'(S658)-IRE1	*P_{tac}-GST-W981F-W1025F-C'IRE1 lacI bla*	Sergej Šesták,
pBS-hXBP1-UN	*P_{T7}-XBP1 splice junction bla*	(Imagawa et al., 2008)

2.1.3 Reagents

Table 3. List of reagents used in this study

Name	Product Number	Company
[α-^{32}P]Adenosine 5'-triphosphate (ATP), 111 TBq (3000 Ci)/mmol	SCP-207	Hartmann Analytic, Germany
[γ-^{32}P]Adenosine 5'-triphosphate (ATP), 111 TBq (3000 Ci)/mmol	SCP-301	Hartmann Analytic
2-Mercaptoethanol	M6250	Sigma-Aldrich, Gillingham, UK
2-Propanol	33539	Sigma-Aldrich
3-[(3-Cholamidopropyl)dimethylam-monio]-1-propanesulfonate (CHAPS)	BIMB1085	Apollo Scientific, Stockport, UK
4-(2-Aminoethyl)-benzenesulphonyl fluoride hydrochloride (AEBSF)	BIMB2003	Apollo Scientific
4-(2-Hydroxyethyl)-1-piperazineethanesulphonic acid (HEPES)	BP310-100	Thermo Fisher Scientific, Loughborough, UK
Acetic acid	A/0360/PB17	Thermo Fisher Scientific
Acrylamide	A8887	Sigma-Aldrich
Acrylamide/bis-acrylamide, 30% solution	A3699	Sigma-Aldrich
Adenosine 5'-diphosphate (ADP), sodium salt (1.5 mol/mol), hydrate	A2383	Sigma-Aldrich
Adenosine 5'-triphosphate (ATP), disodium salt, hydrate (3.5 mol/mol)	A2383	Sigma-Aldrich
Agar	AGA03	ForMedium, Hunstanton, UK
Agarose	MB1200	Melford, Ipswich, UK
Alanine, L-	DOC0104	ForMedium
Ammonium chloride	A9434	Sigma-Aldrich
Ammonium persulfate	BP179-25	Thermo Fisher Scientific
Ampicillin, sodium salt	BIA0104	Apollo Scientific
Arginine, L-	W38,191-8	Sigma-Aldrich
Asparagine, L-	DOC0116	ForMedium
Aspartic acid, L-	DOC0121	ForMedium
Boric acid	B7901	Sigma-Aldrich
Bovine serum albumin	A2153	Sigma-Aldrich
Bromophenol blue	11.439-1	Sigma-Aldrich
1-Butanol	100616J	VWR, East Grinstead, UK
Calcium chloride	C1016	Sigma-Aldrich

Chloramphenicol	BIC0113	Apollo Scientific
Cobaltous chloride hexahydrate	60820	Fluka, Gillingham, UK
Complete protease inhibitor cocktail tablets, EDTA free	11 873 580 001	Roche Diagnostics, Burgess Hill, UK
Coomassie Brilliant blue R-250	BP101-25	Thermo Fisher Scientific
Copper(II) chloride	C3279	Sigma-Aldrich
Ethylenediaminetetraacetic acid (EDTA)	D/0700/53	Thermo Fisher Scientific
Diethyl pyrocarbonate (DEPC)	170250250	Thermo Fisher Scientific
Ecoscint A	LS-273	National Diagnostics
Ethanol, absolute	10100332	Thermo Fisher Scientific
Ethidium bromide	BP102-1	Thermo Fisher Scientific
Formamide	1.04008.2500	VWR
Glucose, D-(+)-	G/0500/61	Thermo Fisher Scientific
Glutamic acid, L-	3510	Calbiochem, Watford, UK
Glutamine, L-	DOC0132	ForMedium
Glutathione, reduced	G1346	Duchefa Biochemie, The Netherlands
Glycerol	G/0650/17	Thermo Fisher Scientific
Glycine	G/0800/60	Thermo Fisher Scientific
Glycogen, RNA grade	R0551	Thermo Fisher Scientific
Guanidine hydrochloride	0118-1KG	Amresco, USA
Histidine, L-	DOC0144	ForMedium
Hydrochloric acid, 37%	10316380	Thermo Fisher Scientific
Iron(III) chloride hexahydrate	F2877	Sigma-Aldrich
Isoleucine, L-	DOC0152	ForMedium
Lactose, α-, monohydrate	L8783	Sigma-Aldrich
LB-agar Lennox	LBX0202	ForMedium
LB-broth Lennox	LBX0102	ForMedium
Leucine, L-	DOC0157	ForMedium
Lysine, L-, hydrate	DOC0161	ForMedium
Lysozyme, from chicken egg white	62971-10G-F	Sigma-Aldrich
Magnesium acetate	0131-500G	Amresco
Magnesium chloride	63068	Fluka
Magnesium sulphate	M/1050/53	Thermo Fisher Scientific
Manganese chloride tetrahydrate	M8054	Sigma-Aldrich
Methanol	M/4000/PC17	Thermo Fisher Scientific
Methionine, L-	DOC0168	ForMedium
N,*N*,*N*',*N*'-Tetramethylethylenediamine (TEMED)	T8133	Sigma-Aldrich
N,*N*'-Methylenebisacrylamide	M7279	Sigma-Aldrich
Nickel(II) chloride hexahydrate	N6136	Sigma-Aldrich
N-Z-Amine A	C0626	Sigma-Aldrich
PageRuler^{TM} Plus Prestained Protein Ladder	26619	Thermo Fisher Scientific

Pepstatin A	BIMI2205	Apollo Scientific
Phenol/Chloroform/Iso-amylalcohol	BP1752-400	Thermo Fisher Scientific
Phenylalanine, L-	DOC0173	ForMedium
Phenylmethanesulphonyl fluoride (PMSF)	MB2001	Melford
Pierce 660 nm protein assay reagent	22660	Thermo Fisher Scientific
Potassium acetate	220150010	Acros Organics, Loughborough, UK
Potassium chloride	P3911	Sigma-Aldrich
Potassium dihydrogen orthophosphate	P/4800/53	Thermo Fisher Scientific
Proline, L-	P0380	Sigma-Aldrich
RNasin	N2111	Promega, Southampton, UK
Serine, L-	DOC0181	ForMedium
Sodium acetate trihydrate	301035K	BDH, East Grinstead, UK
Sodium chloride	S/3120/65	Thermo Fisher Scientific
Sodium dodecyl sulphate (SDS)	161-0301	Bio-Rad, Hemel Hempstead, UK
Sodium hydroxide	28244.262	VWR
Sodium molybdate dihydrate	71756	Sigma-Aldrich
Sodium phosphate, dibasic	S/4520/53	Thermo Fisher Scientific
Sodium phosphate, monobasic	389870010	Acros Organics
Sodium selenite pentahydrate	00163	Fluka
Sodium sulphate	23,931-3	Sigma-Aldrich
Sodium sulphide nonahydrate	208043	Sigma-Aldrich
Sucrose, D-	BPE220-1	Thermo Fisher Scientific
Sulfuric acid, 98%	30325	BDH
Threonine, L-	DOC0185	ForMedium
Tris(hydroxymethyl)-methylamine (Tris)	BI2888	Apollo Scientific
Triton X-100	T/3751/08	Thermo Fisher Scientific
Tryptophan, L-	DOC0188	ForMedium
Urea	AM9902	Ambion, Gillingham, UK
Valine, L-	DOC0197	ForMedium
Xylene cyanol FF	95600	Fluka
Yeast extract powder	YEA02	ForMedium
Zinc sulphate heptahydrate	22,137-6	Sigma-Aldrich
λ protein phosphatase	P9614	Sigma-Aldrich

2.1.4 Solutions for protein work

Table 4. Solutions for protein work

Solution	Composition	Notes
10 x PBS	80 g/l NaCl 2 g/l KCl 14.4 g/l Na_2HPO_4 2 g/l KH_2PO_4	
10 x Protein kinase buffer (Welihinda and Kaufman, 1996)	180 mM HEPES (pH 7.5) 100 mM $Mg(OAc)_2$ 0.5 mM ATP	For each 250 µl of 180 mM HEPES (pH 7.5), 100 mM $Mg(OAc)_2$ add 1.25 µl 100 mM ATP in 1 mM Tris·HCl (pH 8.0)
10 x SDS-PAGE buffer	1.92 M glycine 0.248 M Tris 10 g/l SDS	
6 x SDS-PAGE loading buffer	350 mM Tris·HCl (pH 6.8) 30% (v/v) glycerol 10% (w/v) SDS 0.5 g/l bromophenol blue 2% (v/v) 2-mercaptoethanol	
Coomassie brilliant blue staining solution	0.1% (w/v) Coomassie brilliant blue 50% (v/v) methanol 10% (v/v) acetic acid	
Gel de-staining solution	7% (v/v) methanol 8% (v/v) acetic acid	
Anion exchange start buffer	20 mM Tris-HCl, 1 mM EDTA, 0.5% CHAPS, pH 7.5	
Anion exchange elution buffer	20 mM Tris-HCl, 1 mM EDTA, 0.5% CHAPS, 1 M NaCl, pH 7.5	

2.1.5 Media for *E. coli*

Table 5. Media for *E. coli*

Solution	Composition	Notes
17 aa	10 mg/ml of amino acids (all except for cysteine, tyrosine and methionine)	To make 100 ml: Dissolve 1 g of each of the 17 amino acids in H_2O.
18 aa (Studier, 2005)	7.14 mg/ml of 17 aa 7.14 mg/ml methionine	To make 14 ml: Mix together 10 ml of 17 aa solution and 4 ml of 25 mg/ml methionine
1000 x metals (Studier, 2005)	50 mM $FeCl_3$ 20 mM $CaCl_2$ 10 mM $MnCl_2$ 10 mM $ZnSO_4$ 2 mM $CoCl_2$ 2 mM $CuCl_2$ 2 mM $NiCl_2$ 2 mM Na_2MoO_4 2 mM Na_2SeO_3 2 mM H_3BO_3	To make 100 ml: 50 ml 0.1 M $FeCl_3$ in ~ 0.12 M HCl 2 ml 1.0 M $CaCl_2$ 1 ml 1.0 M $MnCl_2 \cdot 4H_2O$ 1 ml 1.0 M $ZnSO_4 \cdot 7H_2O$ 1 ml 0.2 M $CoCl_2 \cdot 6H_2O$ 2 ml 0.1 M $CuCl_2 \cdot 2H_2O$ 1 ml 0.2 M $NiCl_2 \cdot 6H_2O$ 2 ml 0.1 M $Na_2MoO_4 \cdot 2H_2O$ 2 ml 0.1 M $Na_2SeO_3 \cdot 5H_2O$ 2 ml 0.1 M H_3BO_3 Filter sterilise and store at 20 °C. Autoclave individual metal salt stock solutions except for the 0.1 M $FeCl_3$ solution and store at 20 °C.
25% (w/v) L-aspartate (Studier, 2005)	25% (w/v) L-aspartate	To make 100 ml: 25 g L-aspartate 8 g NaOH Dissolve sequentially in H_2O. Autoclave and store at 20 °C.
50 x 5052 (Studier, 2005)	25% (v/v) glycerol 2.5% (w/v) D-glucose 10% (w/v) α-lactose	Dissolve in H_2O. Filter sterilise. Store at 20 °C.
50 x M (Studier, 2005)	1.25 M Na_2HPO_4 1.25 M KH_2PO_4 2.50 M NH_4Cl 0.25 M Na_2SO_4	Dissolve sequentially in H_2O. Autoclave and store at 20 °C.
LB media	10 g/l tryptone 5 g/l yeast extract 5 g/l NaCl	Dissolve in H_2O. Autoclave. Store at 20 °C.

MDAG-11 plates (Studier, 2005)	25 mM Na_2HPO_4 25 mM KH_2PO_4 50 mM NH_4Cl 5 mM Na_2SO_4 2 mM $MgSO_4$ 0.2 x metals 0.1% glucose 0.1% aspartate 200 µg/ml each of 18 aa 50 µg/ml ampicillin 25 µg/mL chloramphenicol	To make 250 ml: Dissolve 2.5 g agar in ~237 ml H_2O Autoclave. Let cool before adding: 500 µl 1 M $MgSO_4$ 50 µl 1000 x metals 625 µl 40% glucose 1 ml 25% aspartate 5 ml 50 x M 7 ml 18 aa 250 µl ampicillin (50 mg/ml) 125 µl chloramphenicol (25 mg/ml)
MDG (Studier, 2005)	25 mM Na_2HPO_4 25 mM KH_2PO_4 50 mM NH_4Cl 5 mM Na_2SO_4 2 mM $MgSO_4$ 0.5% (w/v) D-glucose 0.25% (w/v) L-aspartate	MDG forms a white precipitate upon storage. It is best to prepare the amount required immediately before use.
ZY media (Studier, 2005)	1% (w/v) N-Z amine A 0.5% (w/v) yeast extract	Dissolve in H_2O. Autoclave. Store at 20 °C.
ZYM-5052 (Studier, 2005)	1% (w/v) N-Z amine AS 0.5% (w/v) yeast extract 25 mM Na_2HPO_4 25 mM KH_2PO_4 50 mM NH_4Cl 5 mM Na_2SO_4 2 mM $MgSO_4$ 0.2 x 1000 x Trace metals 0.5% (v/v) glycerol 0.05% (w/v) D-glucose 0.2% (w/v) α-lactose	To make 500 ml: 479 ml ZY 1 ml Mg_2SO_4 100 µl 1000 x metals 10 ml 50 x M 10 ml 50 x 5052

2.1.6 Solutions for RNA work

Table 6. Solutions for RNA work

Solution	Composition	Notes
10 x TBE	890 mM Tris 890 mM H_3BO_3 20 mM EDTA	Dissolve in DEPC-H_2O. Autoclave
3 M NaOAc (pH 5.2)	3 M NaOAc (pH 5.2)	To make 100 ml: Dissolve 40.83 g NaOAc·3H_2O in ~60 ml DEPC-H_2O. Adjust pH to 5.2 with glacial HOAc Add DEPC-H_2O to 100 ml. Autoclave.
5 M KOAc	5 M KOAc	To make 100 ml: Dissolve 49.07 g KOAc in 90 ml DEPC-H_2O. Add DEPC-H_2O to 100 ml. Add 100 µl DEPC and stir for 30 min at 20 °C. Autoclave
5 x RNA cleavage buffer (adapted from (Imagawa et al., 2008))	100 mM HEPES (pH 7.6) 500 mM KOAc 10 mM $Mg(OAc)_2$	
DEPC-H_2O	H_2O DEPC	To make 1 l: Add 1 ml of DEPC to 1 l of H_2O, stir 30 min at 20 °C. Autoclave.
Gel loading buffer II	95% (v/v) formamide 18 mM EDTA 0.025% (w/v) SDS 0.025% (w/v) xylene cyanol 0.025% (w/v) bromophenol blue	
Phenol:$CHCl_3$:isoamylalcohol, saturated with DEPC-H_2O	Phenol:$CHCl_3$:isoamylalcohol (25:24:1 v/v/v)	
RNA cleavage stop solution	50 mM NaOAc (pH 5.2) 1 mM EDTA 0.1% (w/v) SDS	
RNA elution buffer	50 mM Tris·HCl (pH 8.0) 1 mM EDTA 0.3 M NaOAc	

2.1.7 Solutions for DNA work

Table 7. Solutions for DNA work

Solution	Composition	Notes
10 x TE (pH 8.0)	100 mM Tris·HCl (pH 8.0) 10 mM EDTA	Autoclave for storage
50 x TAE	2 M Tris·HOAc 0.1 M EDTA (pH 8.5)	To make 1 l: 242 g Tris 57.1 ml HOAc 37.2 g $Na_2EDTA \cdot 2H_2O$ Add H_2O to make 1 l

2.1.8 Commercially available kits

Table 8. Commercially available kits

Name	Product number	Company
E.Z.N.A.® Plasmid Midi Kit	D6904-03	Omega Bio-Tek, USA
MEGAscript® T7 High Yield Transcription Kit	AM1333	Thermo Fisher Scientific
Thrombin CleanCleave™ Kit	RECOMT-1KT	Sigma-Aldrich
Wizard® SV Gel and PCR Clean-Up System	A9282	Promega

2.1.9 Special consumables

Table 9. Special consumables

Name	Product number	Company
Amicon Ultra-15 Centrifugal Filter Unit with Ultracel-50 membrane	UFC905008	Merck Millipore
Carestream® Kodak® Bio Max® MS film	Z363006- 50EA	Sigma-Aldrich
Dialysis tubing cellulose membrane	D9777	Sigma-Aldrich
GelAir Cellophane Support	1651779	Bio-Rad
GSTrap 4B	28-4017-48	GE Healthcare, Chalfont St Giles, UK
GSTrap FF	17-5131-02	GE Healthcare
HiTrap Q FF	17-5053-01	GE Healthcare
illustra™ MicroSpin™ S-300 HR Columns	27-5130-01	GE Healthcare Life Sciences
Vacuum Filtration "rapid"-Filtermax, 0.22 µm filters	99255	TPP, Switzerland
Zeba™ Spin Desalting Columns, 7K MWCO, 0.5 ml	89882	Thermo Fisher Scientific

2.2 Methods

Unless stated otherwise, all solutions were prepared in type I laboratory H_2O (resistivity 18 MΩ cm, total organic carbon < 1 ppb, microorganisms < 1 cfu/ml, particles < 0.05 µm diameter) generated using a NANOpure DIamond TOC Life Science ultrapure water system and were autoclaved (121 ºC, 20 min) to sterilise them. All solutions used for chromatography were degassed and particles were removed by filtration over a 0.22 µm filter before use.

2.2.1 *E. coli* culture and plasmid extraction

2.2.1.1 Storage and revival

All *E. coli* strains were stored at -80 ºC in sterile cryo-vials as a mixture of 1 ml of fresh overnight culture and 1 ml of sterile 30% (v/v) glycerol. The XL-10 GOLD strain used for plasmid extraction was revived on LB-agar plates containing 50 µg/ml ampicillin at 37 ºC overnight. The BL21-CodonPlus (DE3)-RIL strain used for protein extraction was revived on MDAG-11 plates (Table 5) (Studier, 2005) containing 50 µg/ml ampicillin and 25 µg/ml chloramphenicol at 37 ºC overnight. To revive the cells, a small droplet of the frozen stock was transferred onto the agar plate and gently spread using a sterile loop next to a Bunsen burner to avoid contamination and obtain single colonies.

2.2.1.2 Plasmid extraction

All plasmid containing cells were grown in LB medium (Table 5) containing 50 µg/ml ampicillin at 37 ºC overnight. pBS-hXBP1-UN, pGEX-1λT-W855F-W981F-C'(S658)-IRE1, pGEX-1λT-W855F-W1025F-C'(S658)-IRE1 and pGEX-1λT-W981F-W1025F-C'(S658)-IRE1 plasmids were extracted using Plasmid Midi kit (Omega Bio-Tek) according to the manufacturer's instructions. Briefly, cells were collected by centrifugation at 3,500 x g at 20 °C for 10 min. Cells were re-suspended in 2.5 ml Solution I/RNase A. 2.5 ml of Solution II was added to the cell suspension and it was incubated at 20 °C for 2 min to obtain a clear lysate. Then, 3.5 ml of Solution III was added and mixed immediately until a precipitate formed. Cells were centrifuged at

23,000 x g at 4 ºC for 30 min to collect cellular debris and genomic DNA. Four ml of the supernatant was transferred into a HiBind® DNA Midi Column and centrifuged at 4,000 x g at 20 °C for 5 min. Three ml of buffer HB was added to the column and centrifuged as before. The plasmids were washed twice with DNA Wash Buffer diluted with ethanol and centrifuged again. Empty columns were centrifuged at 4,000 x g for 10 min to remove residual ethanol. Two ml of the Elution buffer was added to the column and incubated at 20 °C for 2 min. The column was centrifuged for 5 min at 4,000 x g to collect the plasmid. 1/10 volume of 3 M NaOAc (pH 5.2) (Table 6) and 7/10 volume of 2-propanol were added to the plasmid and it was centrifuged at 4 ºC at 23,000 x g for 30 min. The supernatant was discarded, the plasmid was washed once with 70% (v/v) ethanol and re-suspended in the desired amount of 1 x TE (pH 8.0) (Table 7).

2.2.1.3 Plasmid digests

2.2.1.3.1 *Spe*I digest

Restriction enzyme digest is an easy and informative way to confirm the structure and identity of the plasmid (Sambrook and Russel, 2001). pBS-hXBP1-UN plasmid was linearised using *Spe*I enzyme (New England Biolabs) in 1x reaction buffer at 37 ºC overnight. Digest was analysed using agarose gel electrophoresis (described in section 2.2.1.5).

2.2.1.3.2 Proteinase K digest

Proteinase K digests are used to remove contamination from plasmid extracts and have been shown to improve cloning efficiency of PCR products after the digest (Crowe et al., 1991). pBS-hXBP1-UN plasmid was incubated in 1 x TE (pH 8.0) (Table 7) with 100-200 µg/ml Proteinase K in the presence of 0.5% (w/v) SDS at 50 ºC for 30 min. The digest was followed by phenol:$CHCl_3$ extraction and ethanol precipitation.

1 volume of Phenol/$CHCl_3$/Iso-amylalcohol (25:24:1 v/v/v), saturated with 1 M Tris·HCl (pH 8.0) was added to the plasmid. The sample was vortexed to mix the two phases. The mixture was centrifuged at 12,000 x g for 1 min at 20 °C to separate the

phases. The upper phase was carefully transferred into a fresh 1.5 ml microcentrifuge tube avoiding the protein precipitate, which may form between phases. The process was repeated until no more precipitate was observed. The remaining phenolic phases were pooled together and extracted with 0.25 volume of 1 x TE (pH 8.0) (Table 7). The aqueous phases were combined together and 1 volume of $CHCl_3$/iso-amylalcohol (24/1 v/v) was added. The sample was vortexed to mix the phases and centrifuged at 12,000 x g for 1 min at 20 °C to separate them. The $CHCl_3$/iso-amylalcohol extraction was repeated at least once and then upper phase was transferred into a fresh 1.5 ml microcentrifuge tube for ethanol precipitation.

1/10 volume of 3 M NaOAc, pH 5.2 (Table 6) was added to the solution followed by 2.5 – 3 volumes of 100% ethanol. The contents were mixed well and stored o/n (14 to 16 h) at -80 °C. The plasmid was collected by centrifugation at 12,000 x g for 30 min at 4 °C. The pellet was washed with ~200 µl of ice-cold 70% ethanol and centrifuged at 12,000 x g for 15 min at 4 °C. The ethanol was discarded and the plasmid was left to air-dry for 10 – 15 min at 20 °C, re-suspended in desired amount of 1 x TE (pH 8.0) buffer (Table 7) and stored at -20 °C.

2.2.1.4 PCR Spin Column Clean-Up

PCR spin column clean-up was done according to the manufacturer's instructions. Briefly, an equal volume of membrane binding solution was added to the plasmid, all the sample was loaded on the SV Minicolumn and incubated for 1 min at 20 °C. The sample was centrifuged in the SV Minicolumn at 16,000 x g for 1 min at 20 °C. The liquid was discarded. 500 µl of membrane wash solution were added and the sample was centrifuged at 16,000 x g for 5 min at 20 °C. The SV Minicolumn was transferred to a fresh microcentrifuge tube and centrifuged at 16,000 x g for 1 min at 20 °C to evaporate any residual ethanol. The SV Minicolumn was transferred into another sterile microcentrifuge tube, 50 µl of 1 x TE buffer (pH 8.0) (Table 7) were added and incubated for 1 min at 20 °C. The sample was centrifuged at 16,000 x g for 1 min to elute the plasmid. Plasmid concentration was measured using a Nanodrop ND-1000. If necessary, the plasmid was ethanol precipitated and dissolved in smaller amount of 1 x TE buffer (pH 8.0) (Table 7).

2.2.1.5 DNA Agarose gel electrophoresis

Agarose gel electrophoresis is used to separate macromolecules in agarose polymer composed of D-galactose and L-galactose residues joined by two different glycosidic bonds (Sambrook and Russel, 2001). 1% Agarose gels were prepared by mixing the desired amount of agarose with 1 x TAE buffer (Table 7) and microwaving until the agarose had completely dissolved. Once the solution cooled down to ~55 ºC, ethidium bromide was added to the final concentration of 0.5 µg/ml. The gel was poured into a casting unit ensuring that no air bubbles got trapped inside and left to set at 20 °C. 1 x TAE (Table 7) containing 0.5 µg/ml ethidium bromide was used as the running buffer. The voltage applied depended on the size of the gel and the time required (5 V/cm electrode distance). Gels were visualised using a Gel Doc 1000 (Bio-Rad) under UV light illumination (λ_{max} = 300 nm).

2.2.1.6 Transformation of pGEX-1λT plasmids into competent E. coli BL21 CodonPlus (DE3)-RIL cells

BL21-CodonPlus (DE3)-RIL cells contain additional copies of *argU*, *ileY* and *leuW* tRNA genes. The plasmid improves rare codon translation. Many previously published protocols use BL21-CodonPlus (DE3)-RIL competent cells for Ire1 expression (Lee et al., 2008; Valkonen et al., 2004) to improve translation of heterologous proteins coming from organisms with AT-rich genomes.

E. coli cells were transformed using previously published methods (Green and Rogers, 2013). 1-5 µL of plasmid containing solution was added to 50 µl of competent *E. coli* BL21 CodonPlus (DE3)-RIL cells. Cells were incubated on ice for 30 min, heat shocked for 42 s at 42 ºC in a water bath and incubated on ice again for 2 min. One ml of LB medium (Table 5) was added to the cell suspension and it was incubated for 1 h at 37 ºC with shaking at 250 rpm. Cells were plated on LB agar plates containing 50 µg/ml ampicillin and incubated at 37 ºC for 16 h. Positive control was 100 ng of pUC18 plasmid tested before in a transformation. Negative control was 5 µl of 1 x TE (pH 8.0) buffer (Table 7).

2.2.2 Protein Extraction and Purification

2.2.2.1 Protein expression

Previously described methods (Studier, 2005) for protein overexpression using autoinduction were used for Ire1 expression in *E. coli*. Plasmid transformed cells were plated onto MDAG-11 plates (Table 5) containing 50 µg/ml ampicillin and 25 µg/ml chloramphenicol. Plates were incubated overnight at 37 ºC. Three ml of MDG medium (Table 5) containing 50 µg/ml ampicillin and 25 µg/ml chloramphenicol were inoculated with a single colony and grown overnight at 37 ºC with shaking at 260 rpm. 500 ml of ZYM-5052 medium (Table 5) (Studier, 2005) containing 50 µg/ml ampicillin and 25 µg/ml chloramphenicol were inoculated with 500 µl of the saturated culture and incubated for 5 h at 37 ºC with shaking at 220 rpm. The temperature was reduced to 20 ºC and the cultures were incubated for additional 28 h. Cells were collected by centrifugation at 6,000 x g at 4 ºC for 15 min and stored at -20 ºC.

2.2.2.2 Cell lysis

Cells were lysed according to previously described methods (Repaske, 1958; Witholt and Boekhout, 1978). Cell pellets were washed twice in ice-cold 0.2 M Tris-HCl (pH 8.0) and collected by centrifugation at 3,500 x g at 4 ºC for 15 min. Cells were re-suspended in 25 ml lysis buffer [0.2 M Tris-HCl (pH 8.0), 0.5 M sucrose] containing 1 tablet Complete protease inhibitors, EDTA free (Roche Applied Science), 6 mM AEBSF, 1 µg/µl pepstatin and 2 mM PMSF. Ten µg lysozyme/OD_{600nm} dissolved in H_2O to a concentration of 50 mg/ml was used to lyse the cells. Lysozyme was added to the cells and mixed by vortexing. EDTA was added to the final concentration of 1 mM. One volume of H_2O was added to osmotically shock the cells and help the lysozyme penetrate through the bacterial outer membrane. Cells were incubated at 20 °C for 10 min. 1/10 volume of 10% (v/v) Triton X-100 was added and the sample was sonicated (Soniprep 150) at an amplitude of 0.22 microns for 1 min 6 times or until the sample was no longer viscous using the 19 mm Ø probe inserted to a depth of ~ 13 mm. The temperature of the sample was always reduced to 4 ºC between cycles of sonication. The cells were centrifuged at 40,000 x g at 4 ºC for 15 min and the pH of the supernatant was adjusted to 7.4. Lysates were filtered through a 0.22

µm filter using a vacuum pump and a 20 µl sample was retained for SDS-PAGE analysis. Purification was undertaken immediately.

2.2.2.3 Purification by affinity chromatography

Affinity chromatography is based on a reversible interaction between the protein and specific ligand immobilised to a solid phase (Janson, 2012). Two types of columns were used for protein purification in this study: 5 ml GSTrap FF (maximum pressure 70 psi) and 5 ml GSTrap 4B (maximum pressure 42 psi) (GE Healthcare Life Sciences). To prevent from reaching the maximum pressure limits, solutions were pumped through the system at a flow rate of 1 ml/min for GSTrap FF and at 0.5 ml/min for GSTrap 4B. The columns were always connected to the BioLogic DuoFlow™ Chromatography system (Bio-Rad) by first filling the top thread of the column with H_2O to prevent any air bubbles from entering.

2.2.2.3.1 Pre-elution

The column was washed with 5 column volumes of H_2O and equilibrated with 5 column volumes of Equilibration solution (1 x PBS, 5% (v/v) glycerol, 1% (v/v) Triton X-100, 1 mM EDTA). The cell lysate (~25 ml) was loaded onto the column and washed with 5 column volumes of Equilibration solution. The column was then washed with 5 column volumes of Wash solution I (1 x PBS, 5% (v/v) glycerol, 0.1% (w/v) CHAPS, 300 mM NaCl, 1 mM EDTA) and 5 column volumes of Wash solution II (1 x PBS, 5% (v/v) glycerol, 0.1% (w/v) CHAPS, 5 mM $MgCl_2$, 150 mM KCl). Five column volumes of Wash solution II containing 2 mM ATP were used to remove molecular chaperones such as DnaK or HtpG from the fusion protein. DnaK requires Mg^{2+} and K^+ as cofactors, HtpG requires Mg^{2+}. The column was prepared for elution by using 5 column volumes of Elution equilibration solution (1 x PBS, 5% (v/v) glycerol, 0.1% (w/v) CHAPS, 1 mM EDTA). The flow through was collected for each of the wash steps and 20 µl samples were retained for analysis by SDS-PAGE.

2.2.2.3.2 Elution

Protein was eluted from the column using 5 column volumes of elution buffer (20 mM Tris-HCl, 5% glycerol, 100 mM NaCl, 1 mM EDTA, 0.1% CHAPS) containing 10 mM

glutathione. The protein was collected in 1 ml fractions and the protein containing fractions were determined by consulting the UV profile. Two 20 µl samples were retained for analysis by SDS-PAGE and for measuring the concentration using a Thermo Pierce 660 nm protein assay kit.

2.2.2.3.3 Column regeneration

Columns were regenerated by washing them with 5 column volumes of H_2O, 2 column volumes of 6 M guanidine hydrochloride, 5 column volumes of 1 x PBS and 4 column volumes of 70% (v/v) ethanol. Columns were stored in 20% (v/v) ethanol at 4 ºC.

2.2.2.4 Dialysis

2.2.2.4.1 Preparation of dialysis tubing

Dialysis tubing was washed for 3-4 h in running water to remove glycerol. Sulphur compounds were removed by incubating the tubing in 0.3% (w/v) Na_2S at 80 ºC for 1 min. It was then washed with hot water (60 ºC) for 2 min and acidified by immersing briefly in 0.2% (v/v) H_2SO_4. Dialysis tubing was rinsed with hot water to remove any H_2SO_4 and stored in 50% ethanol at 4 ºC.

2.2.2.4.2 Dialysis

1 ml fractions containing the eluted protein were pooled together, transferred into prepared dialysis tubing and dialysed 3 times at 4 ºC against 100 volumes of dialysis buffer (20 mM Tris-HCl, 5% Glycerol, 100 mM NaCl, 1 mM EDTA, 0.025% CHAPS, 1 mM PMSF).

2.2.2.5 Protein concentration

The dialysed protein was concentrated in a 3,000 MWCO ultra centrifugal filter at 3,900 x g at 4 ºC. The concentrators were equilibrated using 10 ml of the elution buffer without glutathione. The protein was transferred into the concentrator and centrifuged until the volume of the upper reservoir reduced to < 1 ml. The remaining protein solution was then transferred into the concentrator and centrifuged until the volume of the upper reservoir reduced to < 300 µl. Five µg of the protein was retained

for analysis by SDS-PAGE and the rest was divided into 20 µl aliquots, snap-frozen in liquid nitrogen and stored at -80 ºC.

The protein concentration was determined using a Thermo Pierce 660 nm protein assay kit according to the manufacturer's instructions and measured in SpectraMax 190 Microplate Reader. The protein standards were produced by dissolving BSA in H_2O at 2 µg/µl and performing 1:2 serial dilutions to make a standard curve from 2 µg/µl to 0.0625 µg/µl. BSA standards were stored at -20 ºC. BSA was chosen as a standard based on previously published protocols (Liu et al., 2002)

2.2.2.6 SDS-PAGE analysis

Polyacrylamide gel electrophoresis (PAGE) is used to separate molecules based on their electrophoretic mobility. The glycine – Tris buffer system in the presence of SDS is the preferred method for analytical separation of proteins (Fling and Gregerson, 1986). SDS unfolds and denatures proteins to form complexes that are mostly defined by a mass-to-charge ratio.

SDS-PAGE gels were made fresh before analysis. Each gel consisted of a stacking gel (4% polyacrylamide) and a separating gel (8% polyacrylamide). The exact composition of each gel layer is described in Table 10. Proteins were mixed with the 6 x SDS-PAGE loading buffer (Table 4), denatured at 100 ºC for 5 min and samples were loaded onto the gel. 120 V were applied for approximately 1.5 h or until the bands reached the bottom of the gel. Proteins were stained using Coomassie Brilliant Blue R250. The gel was stained for 30 min in the staining solution (0.1% Coomassie brilliant blue, 50% (v/v) methanol, 10% (v/v) acetic acid) and destained in 7% (v/v) methanol and 8% (v/v) acetic acid solution until the bands became clearly visible.

Table 10. Composition of SDS-PAGE gel layers.

Component	Separating gel (µl)	Stacking gel (µl)
30% acrylamide, 0.8% bisacrylamide	6000	1010
1 M Tris-HCl, (pH 8.9)	5625	
1 M Tris-HCl, (pH 6.8)		1875
H_2O	9300	4650
10% (w/v) SDS	150	18.75
10% (w/v) APS	130	67
TEMED	30	22

2.2.3 Thrombin cleavage assay

10 µl of thrombin beads (Sigma-Aldrich Thrombin CleanCleave™ Kit) were washed twice using 500 µl of 1 x cleavage buffer (50 mM Tris, 100 mM NaCl, 10 mM $CaCl_2$) by centrifugation at 500 x g for 5 min at 4 ºC. The supernatant was removed and the desired amount of GST-Ire1 protein (up to 500 µg for 10 µl of thrombin beads) together with the desired volume of 1 x cleavage buffer were added to the microcentrifuge tube. Samples were incubated for the desired time (0 h to 24 h as described below in section 3.4.1) at the desired temperature (4 ºC, 20 ºC or 37 ºC as described in section 3.4.1) and centrifuged at 500 x g for 5 min at 4 ºC before taking samples. Samples were stored at -20 ºC before further analysis.

2.2.4 λ protein phosphatase digest

Proteins were de-phosphorylated according to the manufacturer's instructions. ~5 µg of the protein was incubated for 1 h at 30 ºC with 2 µl of 400 U/µl λ protein phosphatase, 2 µl of 10 x λ protein phosphatase buffer [500 mM Tris-HCl, pH 7.5, 1 mM Na_2EDTA, 50 mM dithiothreitol, 0.1% (w/v) Brij 35] and 2 µl of 20 mM $MnCl_2$ in the final volume of 20 µl. Samples were analysed using SDS-PAGE and stained with Coomassie Brilliant Blue.

2.2.5 Anion exchange chromatography

The HiTrap Q FF column was connected to the system preventing any air from bubbles entering the system. The column was washed with 5 column volumes of anion exchange start buffer and 5 column volumes of anion exchange elution buffer at 1 ml/min. The column was then equilibrated with 5 column volumes of the start buffer again. The sample was applied to the system using a syringe and washed with 5 column volumes of the start buffer at 1 ml/min. The proteins were eluted by generating a salt gradient starting from 5 mM NaCl increasing to 1 M NaCl. Protein elution was observed by consulting the UV light absorbance profile. The column was regenerated by washing it with 5 column volumes of elution buffer and 10 column volumes of the start buffer at 1 ml/min.

2.2.6 *XBP-1* splice junction cleavage assay

The RNA cleavage assay was adjusted according to previously published methods (Imagawa et al., 2008). All glassware and spatulas used for this assay were baked at 200 ºC. All buffers and solutions were DEPC-treated and autoclaved or prepared in nuclease-free H_2O. All disposable plasticware was purchased and stored separately for RNA work only to avoid RNase contamination.

2.2.6.1 In vitro transcription reaction

MEGAscript® T7 High Yield Transcription Kit was used for the *in vitro* transcription. The T7 RNA polymerase enzyme mix, 40 U/µl RNasin, 2 U/µl Turbo DNase and the linearised pBS-hXBP1-UN plasmid were thawed on ice. All nucleotide solutions, 10 x reaction buffer and nuclease-free H_2O were pre-warmed to 20 °C. The *in vitro* transcription reaction was assembled in a 1.5 ml microcentrifuge tube by pipetting together the following reagents in the order given below:

To 20 µl Nuclease-free H_2O,
2 µl 10 x reaction buffer,
2 µl 10 mM CTP, 10 mM GTP, 10 mM UTP,
2 µl 1 mM ATP,
1 µl 40 U/µl RNasin,
1 µg linearised pBS-hXBP1-UN plasmid,

1 µl T7 RNA polymerase enzyme mix,
5 µl [α-^{32}P]-ATP (10 mCi/ml, > 3000 mCi/mmol)

The contents were carefully mixed, centrifuged for 10 s at 12,000 x g at 20 °C to collect the reaction mixture at the bottom of the tube and incubated at 37 ºC for 2 h. One µl of 2 U/µl Turbo DNase was added and incubated at 37 ºC for 20 min to remove the DNA template.

2.2.6.2 Purification of the RNA substrate

The RNA substrate was purified according to previously described methods (Rinaldi et al., 2015). A 5% denaturing PAGE gel was prepared by mixing 4.8 g of urea, 1 ml of 10 x TBE (Table 6), 1.7 ml of acrylamide/bis-acrylamide, 30% solution and DEPC-H_2O to the final volume of 10 ml. Once the urea dissolved completely, 80 µl of 10% (w/v) APS and 11 µl of TEMED were added to initiate the polymerisation reaction.

9 µl of nuclease-free H_2O was added to the *in vitro* transcription reaction from 2.2.6.1 to obtain enough volume for gel filtration. Illustra Microspin S-300HR columns were prepared by re-suspending the resin and removing the excess storage buffer by centrifugation at 735 x g for 1 min. The sample was applied to the gel filtration column and centrifuged at 735 x g for 2 min to remove unincorporated nucleotides. The collected sample was mixed with 30 µl of gel loading buffer II (Table 6) and centrifuged at 12,000 x g for 10 s to collect the sample at the bottom of the tube. The sample was denatured at 90 ºC for 5 min and loaded onto a 5% denaturing PAGE gel. 250 V were applied for ~ 25 min or until the bromophenol blue was 0.5 - 1 cm from the bottom of the gel. 1 x TBE (Table 6) was used as a running buffer. The gel was exposed to Carestream® Kodak® BioMax® MS film at 20 °C for 2 min. The RNA containing bands were cut out of the gel and divided into two parts. Each part was chopped into pieces and transferred into a 2 ml screw-cap microcentrifuge tube. 400 µl of RNA elution buffer (Table 6) and 400 µl of phenol:$CHCl_3$:isoamylalcohol (25:24:1 v/v/v), saturated with DEPC-H_2O were added, the tubes were vortexed a couple of times and incubated at 4 ºC overnight.

The samples were vortexed again and centrifuged at 12,000 x g for 1 min. The upper phase was transferred into a new 2 ml screw-cap microcentrifuge tube and 3 volumes of ice-cold 100% ethanol were added. The samples were incubated at -20 ºC overnight. The RNA precipitate was collected by centrifugation at 12,000 x g for 30 min. The pellet was washed with 500 µl of ice-cold 70% ethanol and centrifuged again at 12,000 x g for 15 min. The ethanol was discarded and the RNA was left to air-dry for ~20 min. Each pellet was re-suspended in 60 µl of 1 x TE (pH 8.0) buffer (Table 7) and stored at -20 ºC.

2.2.6.3 Scintillation counting

1 µl of the *in vitro* synthesised RNA was added to 4 ml of scintillation fluid (Ecoscint A) and counted in a scintillation counter (Packard Tri-Carb Liquid Scintillation Analyzer 1600TR) in triplicate. The counts per minute (cpm) detected by scintillation counting were converted into nmols of RNA substrate.

First of all, the counts per minute were converted to disintegrations per minute (dpm) by using a previously determined ^{32}P quench correction curve to which a one phase decay model was fitted.

$$Y = (Y_0 - Plateau) \cdot EXP(-k \cdot X) + Plateau$$

where Y_0 is the Y value when X (time) is zero, $Plateau$ is the Y value at infinite times and k is the decay constant,

$$dpm\ [min^{-1} \cdot l^{-1}] = \frac{cpm\ [min^{-1} \cdot l^{-1}]}{Y \cdot 100}$$

Then, the disintegrations per minute were divided by 60 to obtain a value for disintegrations per second (dps).

The specific activity of [α-^{32}P]ATP added to the reaction is (3000 Ci)/mmol, however, the dilution factor with unlabelled nucleotide must be considered.

The specific activity of the RNA transcript is calculated by the ratio of [α-^{32}P]ATP to unlabelled ATP. Considering that the initial activity of the [α-^{32}P]ATP added to the reaction is (3000 Ci)/mmol, the specific activity is

$$Specific\ activity = \frac{3000\ Ci\ \cdot mmol^{-1}}{n_{ATP}/n_{[\alpha-^{32}P]\mathrm{ATP}}}$$

Where n_{ATP} and $n_{[\alpha\text{-}32P]ATP}$ are moles of unlabeled ATP and labelled ATP respectively.

Once the specific activity is known, the amount of synthesised RNA can be calculated

$$n_{RNA} = \frac{dps\ \cdot V_{RNA}}{Specific\ activity\ \cdot N}$$

Where N is the number of adenylyl nucleotides and V_{RNA} is the volume of RNA added into the scintillation vial.

The measured dps can be converted into Curies (Ci), since $1\ Ci = 3.7\ \cdot 10^{10}\ dps$, which can then be converted into moles of synthesised RNA using the specific activity.

Additionally, the decay factor must be considered because radioactive materials decay according to

$$c = c_0 \cdot e^{-\ln(2)\cdot t/t_{1/2}}$$

Where c is the final activity of radioactive material, c_0 is the initial activity, t is the radiation decay time and $T_{1/2}$ is the isotope half-life.

2.2.6.4 RNA cleavage reaction

A previously published method for *HAC1* mRNA splicing was used (Gonzalez and Walter, 2001), but in this study, *XBP-1* mRNA was used. The cleavage reaction was assembled by pipetting together the following reagents in the following order:

To 30 µl nuclease-free H_2O
6 µl 5 x RNA cleavage buffer (Table 6)
6 µl 10 mM ADP
0.5 µl 40 U/µl RNasin

200 ng GST-Ire1 protein
0.5 nM labelled RNA substrate

The contents were mixed and centrifuged at 12,000 x g for 10 s at 20 °C to collect the sample at the bottom of the tube. Samples were incubated at 37 ºC for 40 min. The reactions were stopped by adding 120 µl of RNA cleavage stop solution (Table 6) and 150 µl of Phenol:$CHCl_3$:isoamylalcohol, saturated with DEPC-H_2O. The samples were vortexed and centrifuged at 12,000 x g for 1 min. The upper phase was transferred into a new 1.5 ml microcentrifuge tube containing 15.4 µl 3 M NaOAc (pH 5.2) (Table 6) and 3.75 µl 2 µg/µl glycogen (RNA grade). Three volumes of ice-cold 100% ethanol were added and the samples were incubated at -20 ºC overnight.

The RNA precipitate was collected by centrifugation at 12,000 x g for 30 min. The pellet was washed with 500 µl of ice-cold 70% ethanol and centrifuged again at 12,000 x g for 15 min. The ethanol was discarded and the RNA was left to air-dry for ~20 min. Each pellet was re-suspended in 15 µl of gel loading buffer II (Table 6), denatured at 90 ºC for 5 min and loaded onto 5% denaturing PAGE gel. 250 V were applied for ~25 min or until the bromophenol blue was 0.5 - 1 cm from the bottom of the gel. 1 x TBE (Table 6) was used as a running buffer. The gel was washed in DEPC-H_2O for 5 min on a shaking platform three times to remove excess urea. The gel was dried between two transparent cellophane support sheets (Bio-Rad) in a GelAir dryer (Bio-Rad) overnight, then exposed to Phosphor Screens (Amersham Biosciences) and visualised using Typhoon 9400 variable mode imager.

2.2.7 Protein kinase autophosphorylation assay

The protein kinase autophosphorylation assay was done according to previously described methods (Welihinda and Kaufman, 1996). The following reagents were pipetted together in the given order:

To 20 µl H_2O
2 µl 10 x protein kinase buffer (Table 4)
5 µg GST-Ire1 protein
1 µl [γ-^{32}P]-ATP (10 mCi/ml, > 3000 mCi/mmol)

The contents were mixed carefully, centrifuged at 12,000 x g for 10 s at 20 °C to collect the sample at the bottom of the tube and incubated at 30 ºC for 30 min. Four µl of 6 x SDS-PAGE loading buffer (Table 4) were added and the sample was denatured at 100 ºC for 5 min. Zeba™ Spin Desalting Columns were prepared for use by removing the bottom closure, loosening the cap and centrifuging at 1,500 x g for 1 min to remove storage solution. The denatured sample was loaded onto the column and centrifuged at 1,500 x g for 2 min to collect the desalted solution. Five µl of 6 x SDS-PAGE loading buffer (Table 4) were added, the sample was denatured again at 100 ºC for 5 min and analysed by SDS-PAGE. The destained gel was dried between two transparent cellophane support sheets (Bio-Rad) in a GelAir dryer (Bio-Rad) overnight, then exposed to Phosphor Screens (Amersham Biosciences) and visualised using Typhoon 9400 variable mode imager.

2.2.8 Safety procedures

2.2.8.1 Handling ethidium bromide

COSHH assessment is required for all procedures that involve handling of more than 10 g of ethidium bromide. Personal protective clothing was used at all times. Gels containing ethidium bromide were disposed in a designated sink fitted with a waste disposal unit. More information about the general safe laboratory practice at the department of Biosciences can be found at

https://www.dur.ac.uk/resources/biosciences/local/SafeLaboratoryPractice.pdf

2.2.8.2 Handling of ^{32}P

Full training was required before working with ^{32}P. Permission to work was issued by the Departmental Radiation Protection Supervisor. All experiments were done in a separate laboratory restricted to “Approved Workers”. All radioactive sources were stored at approved stores (-20 °C freezer or 4 °C fridge). Experiments were carried out in specific work stations. Personal protective clothing was used at all times. Radioactive waste was disposed of via the waste disposal unit. Liquid waste, gels and paper were disposed in the radioactive sink, contaminated solids were washed

extensively until non-radioactive using Decon detergent disposing of the washing as liquid waste. All uses and disposals of radioactive materials were recorded using the usage and disposal record sheets. A full and detailed list of departmental safety procedures can be accessed online at

https://www.dur.ac.uk/resources/biosciences/local/Radiation_Guidelines.pdf

3 Results

3.1 Cloning and transformation of *E.coli* with the constructed plasmids

3.1.1 The tryptophan mutants

pGEX-1λT-W855F-W981F-C'(S658)-IRE1, pGEX-1λT-W855F-W1025F-C'(S658)-IRE1 and pGEX-1λT-W981F-W1025F-C'(S658)-IRE1 plasmids, which were kindly provided by Dr. Sergej Šesták, were successfully transformed into competent *E. coli* BL21 CodonPlus (DE3)-RIL cells. These cells will be referred to hereafter as W855F-W981F-Ire1, W855F-W1025F-Ire1 and W981F-W1025F-Ire1, respectively. All these plasmids encode the cytosolic kinase, RNase and partially truncated linker domains of yeast Ire1 as N-terminal GST-fusion proteins. Specific amino acid substitutions are indicated in the names.

As mentioned above, the plasmids were provided at the start of the project, but all mutagenesis reactions were performed in the pUC18-'*IRE1*'-(*Sac*I-*Hin*dIII) cloning vector. pGEX-1λT-W855F-C'(S658)-IRE1 was generated by cloning the 544 bp *Pml*I-*Sac*I fragment of pUC18-'*IRE1*'-(*Sac*I-*Hin*dIII) into *Pml*I- and *Sac*I-digested pGEX-1λT-(S658)-IRE1. pGEX-1λT-W981F-C'(S658)-IRE1 and pGEX-1λT-W1025F-C'(S658)-IRE1 were generated by cloning the 446 bp *Kpn*I-*Sac*I fragment of pUC18-'*IRE1*'-(*Sac*I-*Hin*dIII) into *Kpn*I- and *Sac*I-digested pGEX-1λT-(S658)-IRE1. Example of the cloning strategy is shown in Figure 3.1. Double mutants were also generated by Dr. Sergej Šesták by successive rounds of QuikChange site- directed mutagenesis (Agilent Technologies).

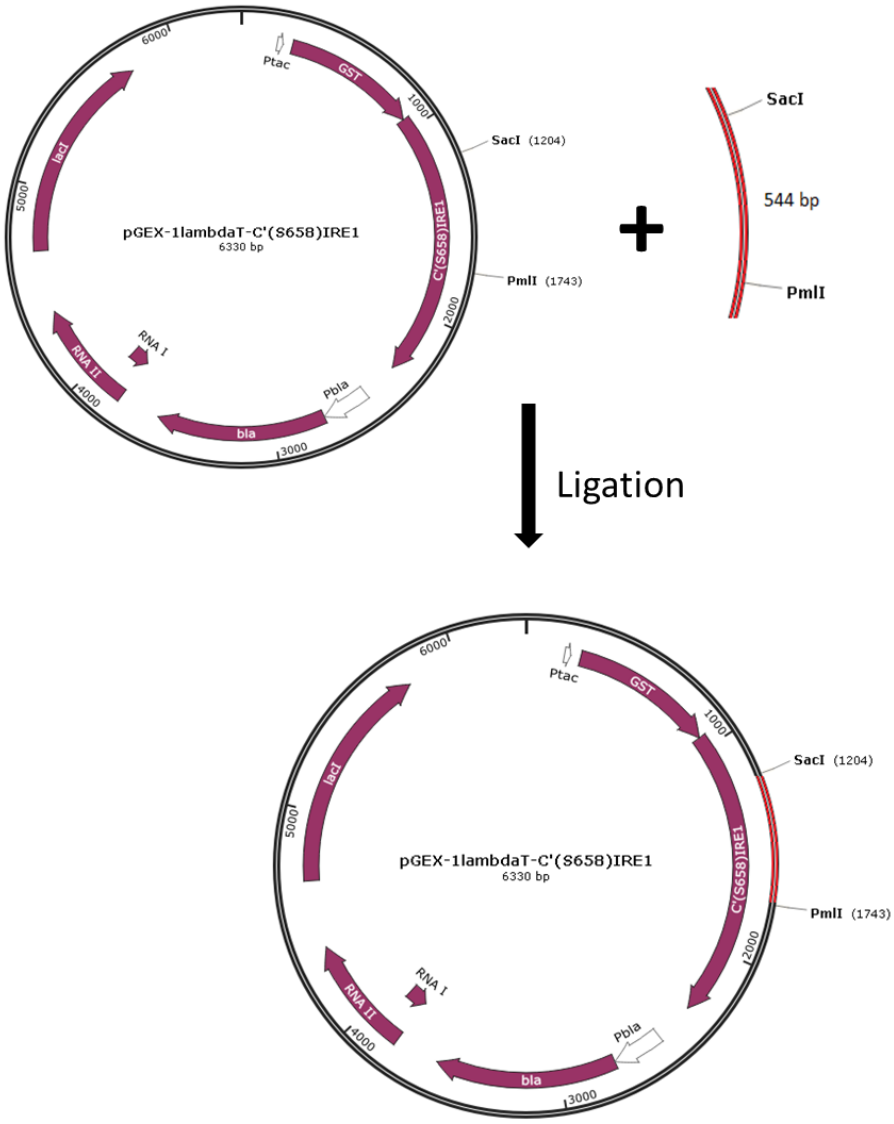

Figure 3.1. Cloning strategy for generating W855F-Ire1
544 bp fragment of *Pml*I-*Sac*I digested pUC18-'*IRE1*'-(*Sac*I-*Hin*dIII) cloned into *Pml*I- and *Sac*I-digested pGEX-1λT-(S658)-IRE1

3.1.2 WT-Ire1 and the kinase mutants

Cells previously transformed by Dr. Martin Schröder including plasmids pGEX-1λT-C'(S658)-IRE1, pGEX-1λT-K799A-C'(S658)-IRE1, pGEX-1λT-N802A-C'(S658)-IRE1, pGEX-1λT-D828A-C'(S658)-IRE1, pGEX-1λT-K799A-N802A-C'(S658)-IRE1, pGEX-1λT-K799A-D828A-C'(S658)-IRE1, pGEX-1λT-K799A-N802A-D828A-C'(S658)-IRE1 and pGEX-1λT-N802A-D828A-C'(S658)-IRE1 will be referred to as WT-Ire1, K799A-Ire1, N802-Ire1, D828A-Ire1, K799A-N802A-Ire1, K799A-D828A-Ire1, K799A-N802A-D828A-Ire1 and N802A-D828A-Ire1 respectively in this thesis. Again, all the plasmids encode the cytosolic kinase, RNase and partially truncated linker domains (starting at the position S658) of yeast Ire1 as N-terminal GST-fusion proteins. An exception is the pGEX-1λT-C'-IRE1 plasmid, which contains the full linker domain, cytosolic kinase and RNase domains. Figure 3.2 shows the structures of the full length yeast Ire1 compared to the cytosolic fraction (C'-IRE1) and the cytosolic part with truncated linker domain (C'(S658)-IRE1). Transformed *E. coli* strains were provided at the start of the project in the form of frozen stocks.

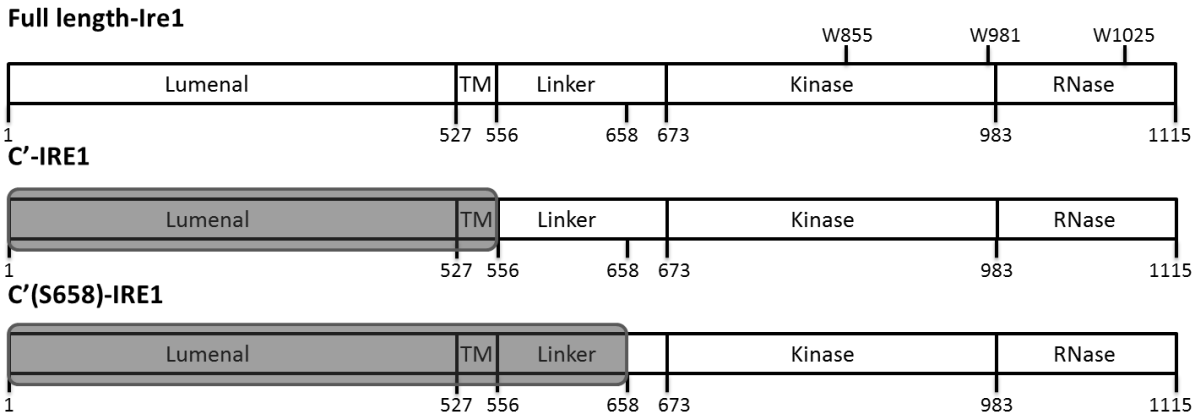

Figure 3.2. Comparison of different fragments of Ire1 used in this study.
Full length yeast Ire1 compared to the full cytosolic fraction (C'-IRE1) and to the cytosolic fraction, which contains partially truncated linker domain (C'(S658)-IRE1). The grey shaded portion was not used for purification. The numbering refers to the amino acids.

3.1.3 Discussion

The goal of this project was to purify and characterise tryptophan mutants. It is difficult to resolve the influence of individual chromophores in proteins that contain various intrinsically fluorescent residues (Beechem and Brand, 1985). A combination of fluorophores results in multiexponential decay making the interpretation of the protein structure and dynamics more problematical, which is potentially the case of Ire1. A promising solution for this is mutating the tryptophan with a non-fluorescent amino acid that has similar structure. Phenylalanine is usually chosen for substituting tryptophan because both have hydrophobic aromatic side chains. However, examples in the literature show that often such substitutions have strong effects on protein structure and functions. For example, in the case of bacteriorhodopsin, some tryptophan substitutions result in blue shifts in the chromophore and impaired proton pumping (Mogi et al., 1989). Two out of eight tryptophan residues are also crucial for the function of yeast eIF-4E (Altmann et al., 1988). Therefore, the mutants must first be characterised before use in fluorescence studies.

3.2 Protein purification

3.2.1 Purification using affinity chromatography

In this study, GST-fusion proteins were expressed by autoinduction (Studier, 2005) using previously determined optimal conditions (Schröder, unpubl.) and purified using affinity chromatography on GSTrap 4B or GSTrap FF columns. Affinity chromatography is based on the ability of a protein to covalently bind to a specific matrix. When an impure protein solution is passed through this matrix, the protein binds to it while most of the impurities are washed away with the buffer. The protein is then recovered by changing the elution conditions so that the protein gets released from the chromatographic material. In the case of Ire1 used here, the plasmid construct contains a GST tag which is known for high affinity to glutathione. Autoinduction is based on the ability of certain media to induce protein expression in *E. coli* once the cells reach saturation. Cells use glucose as the initial energy source until mid to late log phase. Upon glucose depletion, cells start to use lactose and convert it into inducer allolactose. The stage of induction can be regulated by the levels of glucose and lactose in the media. Using auto-induction was shown to produce higher protein yields. Theoretically, 500 ml of starting culture should produce ~50 mg of protein. However, we have never recovered >20 mg.

The cells were successfully lysed and loaded onto the columns where the GST-tagged protein efficiently and reversibly binds the matrix. After several wash steps the protein interaction with the matrix was reversed using 10 mM glutathione and the eluted protein was dialysed as described in Materials and Methods. Figure 3.3 shows an SDS-PAGE gel corresponding to the purification of WT-Ire1. Each lane represents a step in the purification process as indicated above the gel. The last lane shows the final dialysed protein (~5 µg).

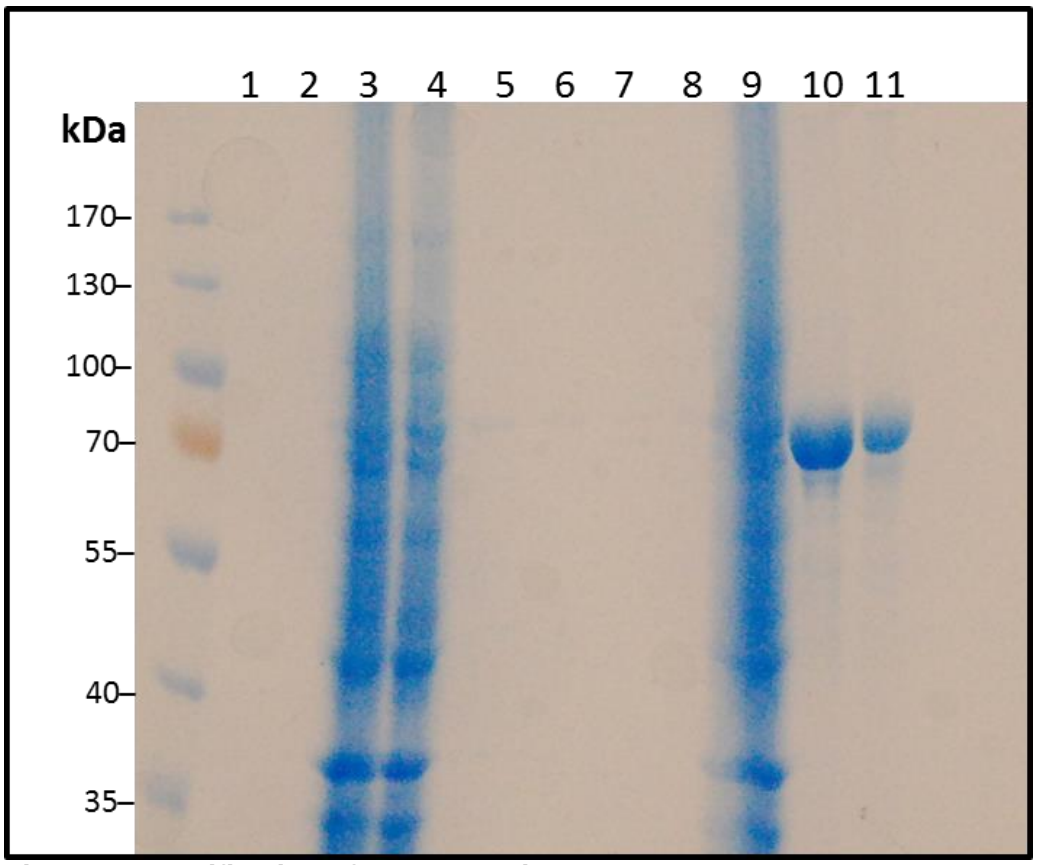

Figure 3.3. Purification of GST tagged WT-Ire1.
Each lane represents a sample of the collected flowthrough during the process of WT-Ire1purification by affinity chromatography. The column was washed with H_2O (lane 1) to remove any excess ethanol and equilibrated with equilibration solution containing 1% Triton X-100 (lane 2). After loading of the lysed cells (lane 3), column was washed with the same equilibration solution to remove any unbound protein (lane 4). The column was then washed with Wash solution I containing 300 mM NaCl (lane 5) and Wash solution II containing 5 mM $MgCl_2$ and 150 mM KCl (lane 6). The last wash step was done with Wash solution II containing 2 mM ATP (lane 7) to remove molecular chaperones. The column was equilibrated before elution (lane 8). Lane 9 contains 20 µl of the lysed cells that were loaded onto the column. Lanes 10 and 11 represent the purified protein before and after dialysis respectively.

Initially, seven proteins were purified and used for analysis including the WT-Ire1, three tryptophan mutants and three kinase mutants, namely K799A-N802A-Ire1, K799A-D828A-Ire1 and K799A-N802A-D828A-Ire1. Figure 3.4 shows an SDS-PAGE gel image with ~5 µg of each purified protein (names indicated above the lanes). The purification protocol was optimised for the wild type protein, therefore it purifies as a full length single band. Other proteins do not purify as well as the WT-Ire1. Out of the tryptophan mutants, only the W855F-W1025F-Ire1 is seen as a single band of a similar sized protein to WT-Ire1. The W855F-W981F-Ire1 purifies as two strong bands

probably corresponding to a full length protein and a truncated version. The W981F-W1025F-Ire1 has a much fainter band of the size of the full length protein and a strong band corresponding to a slightly smaller protein. Again, a plausible explanation is that the lower band corresponds to a truncated protein. The two bands may also be a result of different phosphorylation states of the protein (see chapter 3.2.2). Some additional bands were observed at the bottom of the gel for the tryptophan mutants, potentially either smaller size impurities or truncated bits. K799A-N802A-Ire1 purifies as well as the WT-Ire1 and migrates slightly further on a gel indicating a smaller size protein, potentially due to lack of phosphorylation. Other kinase mutants, both K799A-D828A-Ire1 and K799A-N802A-D828A-Ire1 also migrate further than the wild type protein and have visible impurities.

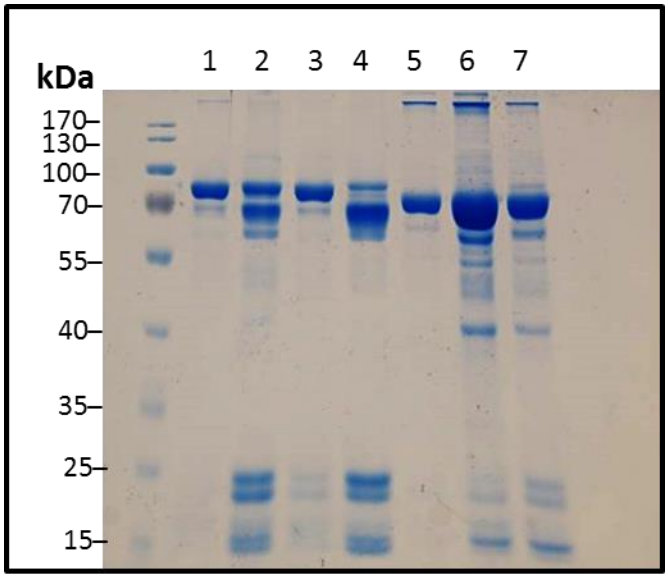

Figure 3.4. Purification of WT-Ire1 and different mutant proteins.
~5 µg of each of the purified proteins were subjected for analysis by SDS-PAGE: WT-Ire1 (lane 1), W855F-W981F-Ire1 (lane 2), W855F-W1025F-Ire1 (lane 3), W981F-W1025F-Ire1 (lane 4), K799A-N802A-Ire1 (lane 5), K799A-D828A-Ire1 (lane 6), K799A-N802A-D828A-Ire1 (lane 7).

3.2.2 λ phosphatase digest

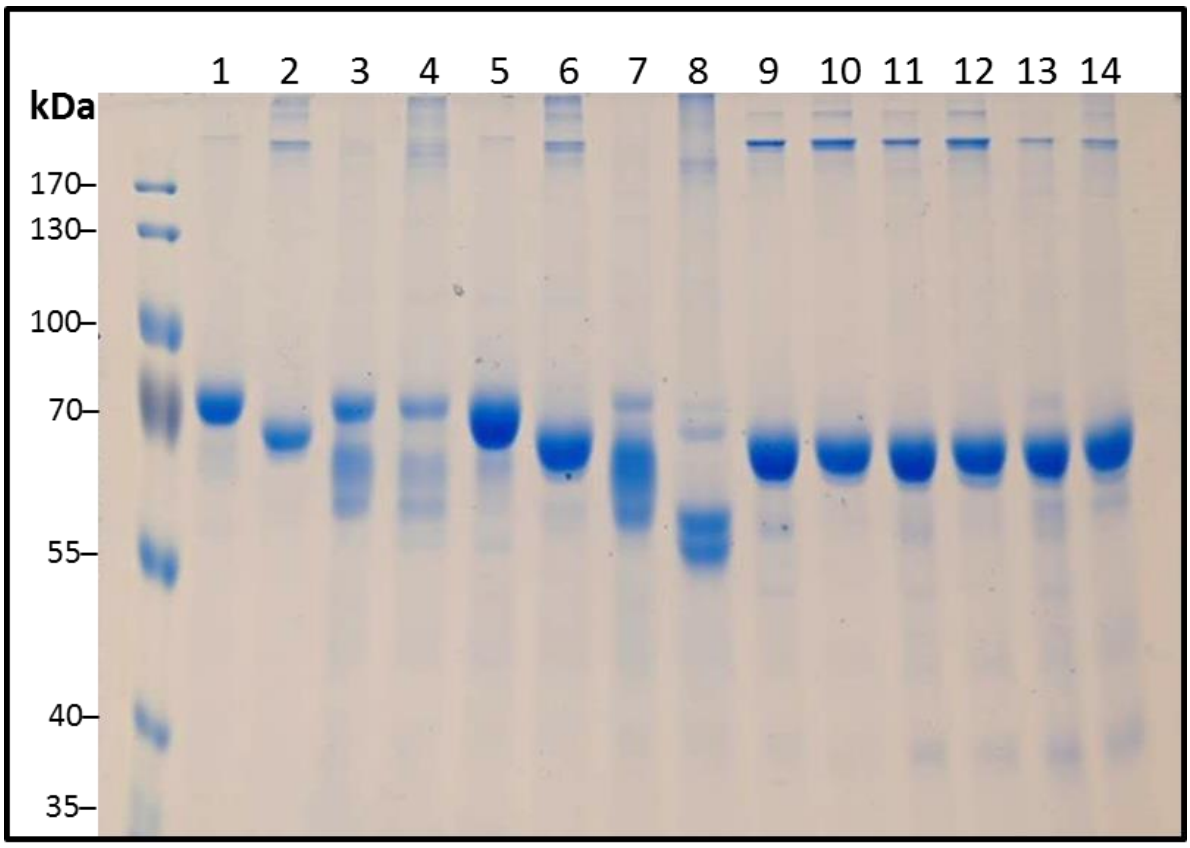

Figure 3.5. λ phosphatase digest of the seven initially purified proteins.
~5 µg of the GST-fusion proteins were subjected to a λ phosphatase digest. WT-Ire1 undigested (lane 1) and digested (lane 2), W855F-W981F-Ire1 undigested (lane 3) and digested (lane 4), W855F-W1025F-Ire1 undigested (lane 5) and digested (lane 6), W981F-W1025F-Ire1 undigested (lane 7) and digested (lane 8), K799A-N802A-Ire1 undigested (lane 9) and digested (lane 10), K799A-D828A-Ire1 undigested (lane 11) and digested (lane 12), K799A-N802A-D828A-Ire1 undigested (lane 13) and digested (lane 14).

First, we ruled out the initial hypothesis that the two bands observed on the gels for W855F-W981F-Ire1 and W981F-W1025F-Ire1 may be a phosphorylated and a non-phosphorylated form of the same protein. Proteins were tested by digesting them with λ protein phosphatase (λ PP). The enzyme removes phosphate groups from phosphorylated serine, tyrosine and threonine residues. Figure 3.5 shows all seven initially purified proteins in their undigested form and the same proteins after the λ phosphatase treatment. The assay shows that all kinase mutants show no difference in migration after the digest suggesting that the kinase mutations have an effect in the autophosphorylation ability of these proteins and they purify in a non-phosphorylated form. The WT-Ire1 purifies as a phosphorylated protein and the phosphates can be

removed resulting in a similar sized protein to the kinase mutants (compare WT + λ PP and all six lanes corresponding to the K799A mutants). W855F-W1025F-Ire1 behaved similarly to WT-Ire1. W981F-W1025F-Ire1, which does not purify as a single full length protein, retains additional bands on the gel after the λ phosphatase digest, suggesting that the two bands must represent different proteins rather than different forms of phosphorylation. Curiously, W855F-W981F-Ire1 was not affected by λ phosphatase digest. This behavior was unexpected and hard to explain, therefore, additional experiments were done to confirm that something went wrong with the digest.

Figure 3.6 shows gel images of the repeated λ phosphatase digest. Gel A shows all the proteins in the absence of λ phosphatase and gel B shows the same proteins digested with λ PP. The gels show that the W855F-W981F-Ire1 mutant can be de-phosphorylated because it migrates in the same way as WT-Ire1 in both phosphorylated and non-phosphorylated form. The only issue with this experiment is that all the proteins should have been loaded on the same gel again. However, before λ phosphatase digest, the WT-Ire1 and other proteins run above the 70 kDa band and after the digest they all run below the band indicating, that the digest most likely had worked. This result suggests that the tryptophan mutations do not have an effect on the ability of Ire1 to autophosphorylate and that the purification protocol optimised for the wild type protein may not be ideal for purifying other mutants.

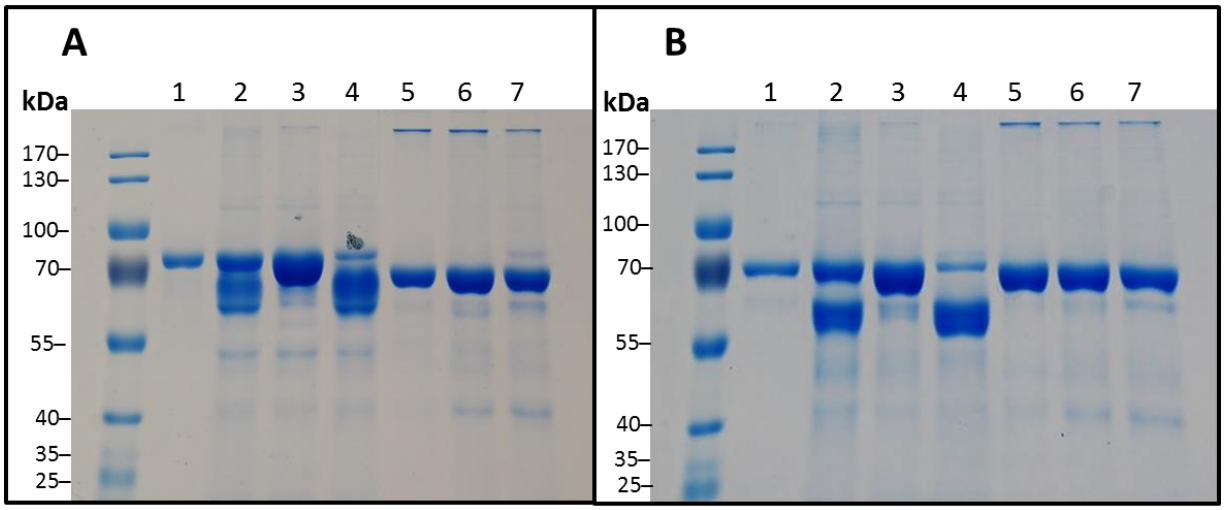

Figure 3.6. Repeated λ phosphatase digests.

A. ~5 µg of undigested GST-fusion proteins.

B. ~5 µg of the GST-fusion proteins digested with λ protein phosphatase.

Proteins were loaded in the following order: WT-Ire1 (lane 1), W855F-W981F-Ire1 (lane 2), W855F-W1025F-Ire1 (lane 3), W981F-W1025F-Ire1 (lane 4), K799A-N802A-Ire1 (lane 5), K799A-D828A-Ire1 (lane 6), K799A-N802A-D828A-Ire1 (lane 7).

It is possible that the mutant proteins need different expression conditions to fold properly. W855F-W981F-Ire1 was tested in different induction conditions. A smaller culture was grown for 5 h at 37 ºC and after reducing the temperature to 20 ºC samples were taken after 20 h, 22 h, 24 h, 26 h, 28 h, 30 h and 32 h. Cells were lysed and incubated with glutathione sepharose 4B beads (GE healthcare). The beads were washed, mixed with 6 x SDS-PAGE loading buffer, denatured and analysed by SDS-PAGE. All different time points retained the two bands (data not shown) suggesting that either that protein needs even more different induction conditions (lower temperature, different pH) or alternatively, the mutations may cause ribosomes to fall off prematurely during translation giving rise to a truncated product.

3.2.3 Discussion

The initial purification results suggest that the aim to purify functional tryptophan mutants may be more challenging than initially expected. The purification protocol has been optimised on WT-Ire1 and tested in the past with a variety of kinase mutants. As observed in the past and also in the results presented here, the kinase mutants purify fairly well as single condensed bands. Of course, the observations in this case are based on the gel image. However, in the case of the tryptophan mutants, only one of them (W855F-W1025F-Ire1) purifies as a single protein, while the other two most likely purify as mixtures of full length and truncated versions of the proteins. The results obtained here support this idea, but mass spectrometry analysis would be helpful to determine what the two bands are. If the proteins are truncated at the C-terminus, they probably lack the whole RNase domain, which may present problems in obtaining mRNA splicing activity.

The truncated proteins may be generated by the ribosomes falling off prematurely during translation or by proteases. In the first case, it may be necessary to further optimise induction conditions for purifying mutant proteins by adjusting the temperature or pH. In the second case, switching to a different *E. coli* strain for purification may solve the problem.

Since the tryptophan residues are in different parts of the protein, it would be interesting to look at all of them using fluorescence spectroscopy. Therefore, all the mutants were retained for the analysis and characterisation of the kinase and RNase activities instead of spending months trying to first optimise the purification conditions.

3.3 Characterisation of the RNase and kinase activity of the tryptophan mutants

3.3.1 Optimising the RNA labelling reaction

The RNase (endoribonuclease) domain of Ire1 initiates a non-conventional splicing reaction producing a potent UPR transcription activator. XBP-1 is the best studied mRNA substrate for Ire1 cleavage activity. It is a direct target for Ire1 endoribonucleolytic activity (Calfon et al., 2002) and contains two overlapping open reading frames (Nekrutenko and He, 2006). Activated Ire1 removes a 26 nucleotide intron and generates a frame shift to produce active XBP-1. *In vitro*, Ire1 activity can be measured by synthesizing XBP-1 mRNA, incubating it with the protein and analyzing the samples on a denaturing PAGE gel. If the protein retains endonuclease activity, four cleavage bands will be observed on the gel. Figure 3.7 A shows a schematic representation of the unspliced (XBP1u) and spliced (XBP1s) forms of full length XBP-1 mRNA. In the presence of tRNA ligase, a functional transcriptional activator is generated after removal of 26 nt. The plasmid used in the assay encodes the splice junctions and intron only. The XBP-1 splice sites form very similar stem-loop structures to yeast HAC 1 mRNA (Yoshida et al., 2001), therefore, the fragment used in this study can be cleaved using yeast protein. Part B of Figure 3.7 shows the splicing products, which can be observed on a denaturing PAGE gel in the absence of the tRNA ligase. The 26 nt intron is probably too small to be visualised.

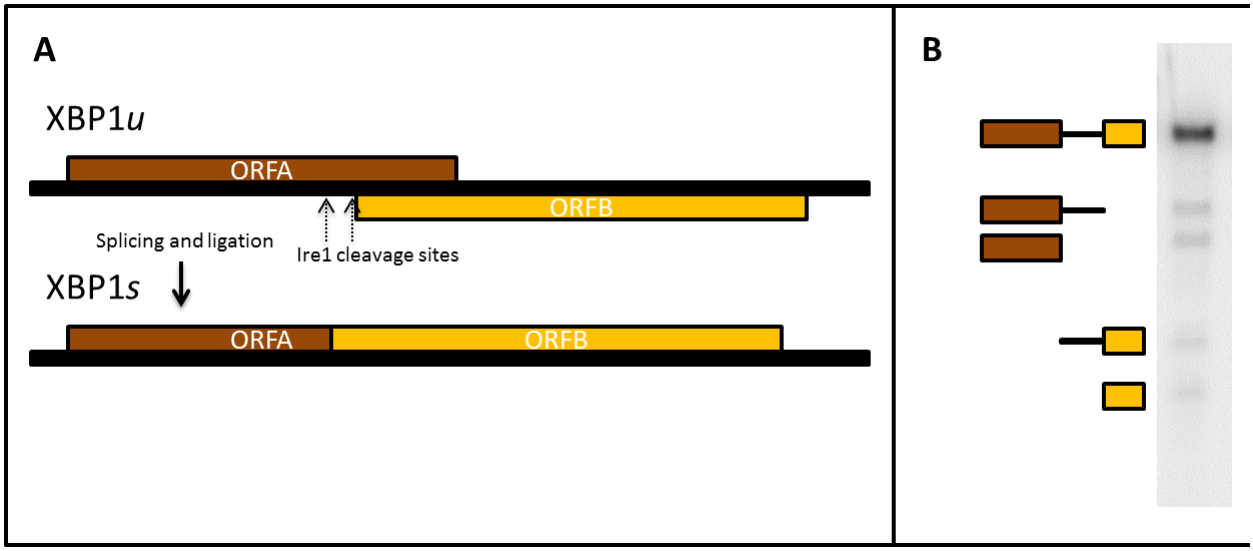

Figure 3.7. The structure of XBP-1 mRNA.

A. Inactive XBP-1 has two overlapping open reading frames. Small arrows show specific Ire1 cleavage sites, which are separated by 26 nt. Splicing and removal of this fragment generates a frame shift and produces a functional transcriptional activator.

B. XBP-1 mRNA cleavage by Ire1 produces five mRNA fragments, four of which can be visualised on a denaturing PAGE gel.

The initial attempts to generate RNA substrate were unsuccessful. An old *in vitro* transcription kit (purchased two years ago) was used in this case and the plasmid was extracted using the plasmid Midi kit. The gels exposed to autoradiography films had very faint or no bands suggesting that very few or no radioactively labelled nucleotides were incorporated into the RNA transcript and indicating that the reaction had not worked. The synthesis was repeated with a new *in vitro* transcription kit and freshly prepared materials, but unfortunately, it failed again. One of the few remaining explanations for repeated failure was potential cross contamination coming from the plasmid preparation, which may inhibit the RNA polymerase. The pBS-hXBP1-UN was successfully isolated using a plasmid extraction kit and linearised using the *Spe*I enzyme. The attempt to use the plasmid prepared in this way resulted in very low yields of the RNA transcript, therefore, the plasmid was digested with proteinase K to remove any impurities before using it for the labelling reaction. Proteinase K is a broad spectrum serine protease commonly used to remove any contaminating proteins, especially the RNases. Digesting protein impurities in the plasmid DNA sample with proteinase K followed by phenol:$CHCl_3$ extraction and ethanol precipitation did not solve the problem either. However, proteinase K needs the

presence of a detergent such as SDS to denature the proteins and make the hydrophobic amino acid residues accessible for cleavage. The carry-over SDS in the plasmid preparation is likely to inhibit the T7 RNA polymerase resulting in low yields of labelled RNA substrate. Doing a PCR clean-up step to remove the traces of SDS solved the issue and resulted in constant and reliable labelled RNA synthesis. Figure 3.8 A shows an example of high yield RNA synthesis and Figure 3.8 B shows a low yield *in vitro* transcription as observed by exposing the gel to autoradiography film for 2 min.

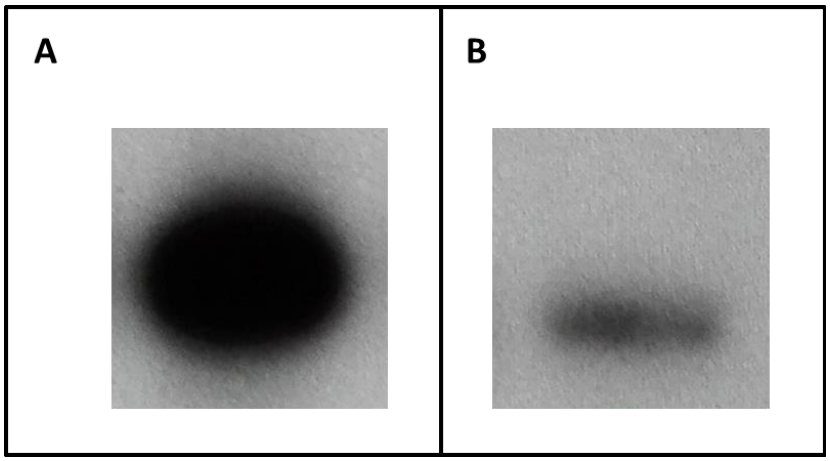

Figure 3.8. Comparison of high yield and low yield *in vitro* XBP1 mRNA labelling reaction.

A. Gel exposed to autoradiography film for 2 min indicates successful RNA labelling.

B. Gel exposed to autoradiography film for 2 min indicates poor RNA synthesis.

3.3.2 All tryptophan mutants retain protein kinase activity

In order to do spectroscopy studies on the tryptophan mutants they must first be tested for activity. Only those proteins that retain both their kinase and RNase activity can be used as reliable models for such analysis. Depending on their type, kinases transfer the γ phosphate from ATP onto serine and threonine or tyrosine residues on target proteins. In some cases, the protein kinases can be dual-specificity and phosphorylate both serine/threonine and tyrosine residues (Lindberg et al., 1992). *In vitro*, protein kinase activity can be measured as the incorporation of radiolabeled phosphate from [γ-^{32}P]ATP into a protein substrate. In the case of Ire1, autophosphorylation is observed by incubating the protein with [γ-^{32}P]ATP and

analyzing the proteins by SDS-PAGE. Only those proteins that retain kinase activity will have detectable bands using autoradiography.

Figure 3.9 shows photos for the same gel stained with Coomassie brilliant blue (A) and imaged for radioisotope detection (B). The images show that the WT-Ire1 and all tryptophan mutants have visible bands on the phosphoimager scan and therefore have some kinase activity. The K799A-N802A-D828A-Ire1 mutant has a very faint band indicating lack of activity. It also works as a negative control for this study because of previous observations that kinase mutations inhibit the autophosphorylation of Ire1 (Rubio et al., 2011). The bands were quantified by dividing the intensity of the bands detected by phosphoimager by the intensity of the Coomassie staining. The obtained values were converted into percentage and the activity of each mutant was compared to WT-Ire1. Nevertheless, the assay has certain limitations given that the proteins may be purified in their phosphorylated forms and cannot incorporate all of the available radioactive phosphate. Figure 3.10 shows the quantification assuming that the WT protein has 100% kinase activity. W855F-W981F-Ire1 purifies as two bands, so these two bands were quantified individually. Separately, they have reduced activity compared to WT-Ire1, but together W855F-W981F-Ire1 seems to be more active. W855F-W1025F-Ire1 purifies nicely as a single protein and has ~50% activity of the WT-Ire1 protein. As observed in Figure 3.9, W981F-W1025F-Ire1 has very low intensity staining with Coomassie, but a bright band for the ^{32}P detection. Quantification of bands gave ~120% activity compared to WT-Ire1. K799A-N802A-D828A-Ire1 is a kinase mutant, which was used as a negative control for the experiment gave <5% activity.

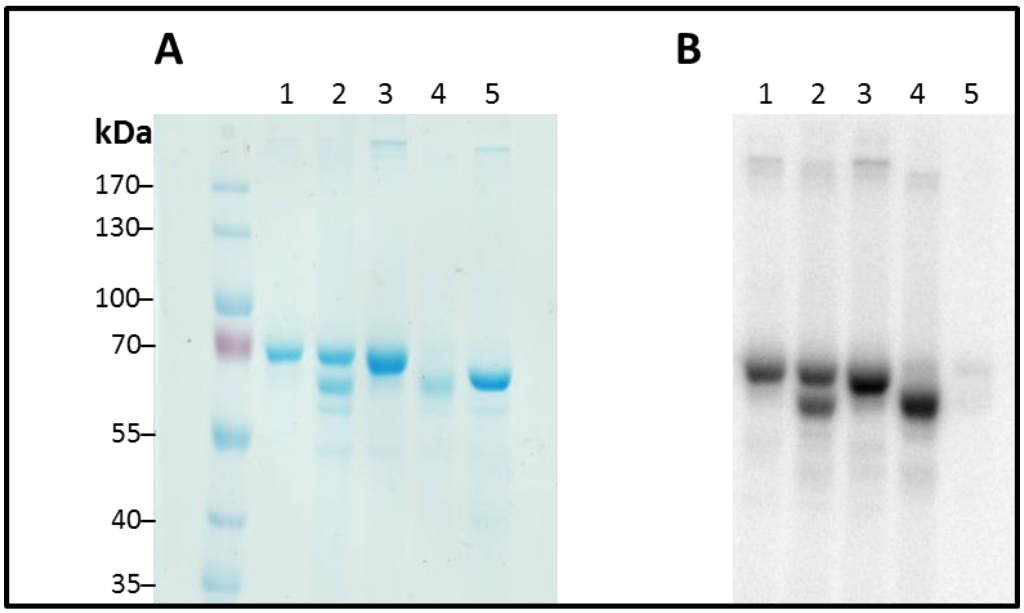

Figure 3.9. WT-Ire1 and all tryptophan mutants retain kinase activity.
Example image of a kinase assay gel stained with Coomassie and then exposed to autoradiography imager.

- **A.** Coomassie brilliant blue staining of ~5 µg of loaded protein.
- **B.** ^{32}P radioisotope detection using Typhoon 9400 variable mode imager.

Proteins were loaded in the following order: WT-Ire1 (lane 1), W855F-W981F-Ire1 (lane 2), W855F-W1025F-Ire1 (lane 3), W981F-W1025F-Ire1 (lane 4), and K799A-N802A-D828A-Ire1 (lane 5).

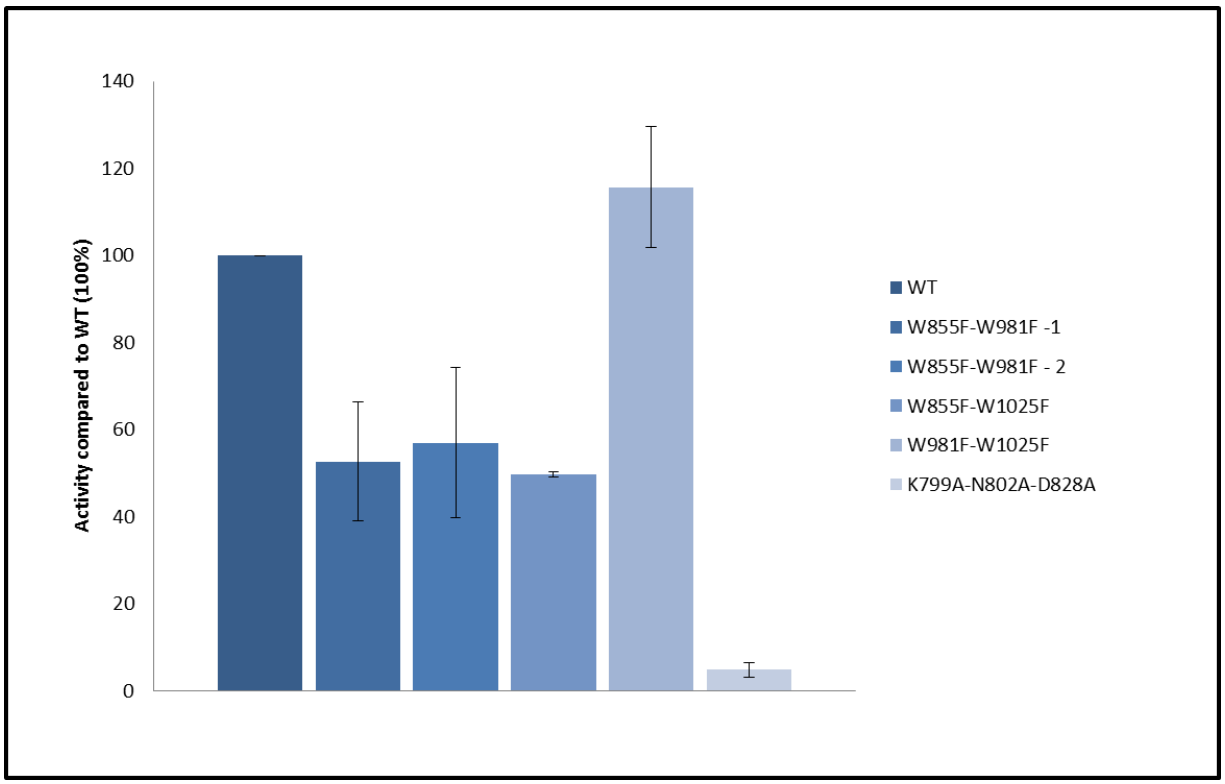

Figure 3.10. Quantification of kinase activity for the tryptophan mutants.
The intensity of Coomassie staining was compared to the intensity of the phosphoimager scan and compared to the WT-Ire1 assuming that the wild type protein is 100% active. The two bands for W855F-W981F-Ire1 (Figure 3.9) were quantified individually. For W981F-W1025F-Ire1 (Figure 3.9), only the intensive bottom bands were quantified. Values are averages of two repetitions ±SEM.

3.3.3 Only W855F-W981F-Ire1 retains RNase activity

Once the *in vitro* transcription reaction was optimised, the tryptophan mutants were assessed for activity. Proteins were incubated with the RNA substrate in the presence of RNA cleavage buffer. RNasin was also used to prevent possible RNA degradation. No nucleotide, ATP and ADP were tested with each protein to optimise the RNA cleavage assay protocol. After the incubation, reactions were stopped using RNA cleavage stop solution followed by phenol:$CHCl_3$ extraction and ethanol precipitation using glycogen as a carrier to recover the RNA. The RNA was then subjected for analysis on a denaturing PAGE gel. Figure 3.11 shows the results of this assay. The control lane contains only the RNA substrate and works as a negative control while the WT-Ire1 was used as a positive control. All proteins were incubated for 40 min in the absence of nucleotide, with ATP and with ADP. The results for WT-Ire1 indicate that nucleotide binding is essential for RNase activity. Therefore, in the future experiments ADP was always used as the nucleotide for RNA cleavage assay. Unexpectedly, the W855F-W1025F- Ire1 mutant, which purifies as a full length protein does not seem to retain any RNase activity. The only mutant showing some cleavage is the W855F-W981F-Ire1. The bands are less intense than for the WT-Ire1, which may be attributed to only a fraction of the protein mixture being active.

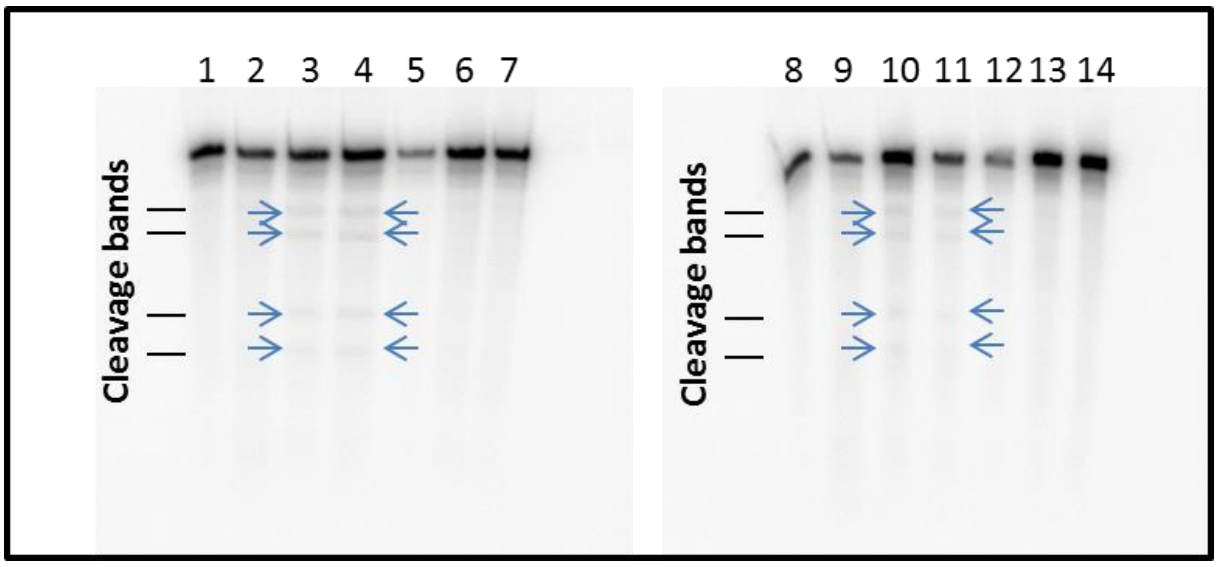

Figure 3.11. Only one tryptophan mutant retains RNase activity.
Nucleotide binding is essential for RNase activity and only one of the tryptophan mutants (W855F-W981F-Ire1) retains some activity. The blue arrows show cleavage bands. The samples were loaded in the following order: RNA substrate only (lane 1 and 8), RNA + WT-Ire1 (lane 2), RNA + WT-Ire1 + ATP (lane 3), RNA + WT-Ire1 + ADP (lane 4), RNA + W855F-W1025F-Ire1 (lane 5), RNA + W855F-W1025F-Ire1 + ATP (lane 6), RNA + W855F-W1025F-Ire1 + ADP (lane 7), RNA + W855F-W981F-Ire1 (lane 9), RNA + W855F-W981F-Ire1 + ATP (lane 10), RNA + W855F-W981F-Ire1 + ADP (lane 11), RNA + W981F-W1025F-Ire1 (lane 12), RNA + W981F-W1025F-Ire1 + ATP (lane 13), RNA + W981F-W1025F-Ire1 + ADP (lane 14).

3.3.4 Discussion

Overall, this chapter describes the activity of the initially purified proteins in terms of their ability to autophosphorylate and process mRNA. Results for the kinase assay suggest that all tryptophan mutants retain at least partial kinase activity. The kinase assays are probably more qualitative than quantitative because of the limitations arising. In order to fully determine how active each mutant is, analysis of the enzyme kinetics should be done (Wang and Wu, 2002). However, in this study, the selected assay showed that the mutants have at least some kinase activity and theoretically should be usable for the fluorescence spectroscopy studies.

In terms of the RNase activity, the results showed potential limitations. The mutant, which purifies well seems to have lost RNase activity. This is not surprising because one of the mutated tryptophan residues (W1025) is in the RNase domain and may be essential for its function. Interestingly, the W855F-W981F-Ire1 shows some cleavage activity, which may be explained by the fact that both mutations are in the kinase domain and therefore do not need to affect the catalytic function. Nevertheless, the problem with this particular mutant as described in the protein purification chapter is that it purifies as two individual proteins, one of them potentially lacking the RNase domain. The results could be interpreted in a way, that the full length W855F-W981F-Ire1 retains full RNase activity, while the truncated portion lacks any. If this is the case, the concentration of active protein in the assay is lower than in the WT-Ire1, resulting in more faint bands.

There is a possibility that contamination during RNA synthesis may affect protein RNase activity. However, WT was used as a positive control for the experiments and in the case of contamination it would be unlikely to see any cleavage bands for WT-Ire1. Since the RNA substrate used for activity studies is the same for all proteins, mRNA cleavage should be observed for active mutants as well.

3.4 Optimisation of the thrombin cleavage and characterisation of the RNase and kinase activity of the cleavage products

3.4.1 Optimising the thrombin cleavage assay

Thrombin is a protease used for GST tag removal from proteins expressed from pGEX vectors containing a recognition sequence for thrombin. pGEX-1λT is one of these vectors, therefore, thrombin was used in this study for GST cleavage. WT-Ire1 was used for optimising the cleavage assay. Different temperatures including 4 ºC, 20 ºC and 37 ºC were tested over the time course of 24 h. Figure 3.12 shows gel images for thrombin cleavage assay over time at 4 ºC, 20 ºC and 37 ºC. The bands were also quantified using ImageJ and cleavage efficiency was calculated by dividing the amount of protein cleaved by the total amount of protein. The results are shown in Figure 3.13. These figures indicate that thrombin is inactive at 4 ºC but active at both 20 ºC and 37 ºC. The protein is digested faster and more fully at 37 ºC reaching >90% cleavage in less than 4 h, whereas at 20 ºC, >24 h are needed to achieve that. However, Ire1 is not very stable at higher temperatures so 24 h at 20 ºC was selected as the optimal temperature for cleavage to avoid exposing the protein to high temperature and still obtain a reasonably fast and efficient cleavage.

As described in the cloning and transformations chapter and shown in Figure 3.2, two different constructs of Ire1 were used in this study. For thrombin cleavage at 4 ºC, the shorter fragment (C'(S658)-Ire1) was used, whereas for 20 ºC and 37 ºC, the longer fragment (C'-Ire1) was used. The result of that can be observed on the gels in Figure 3.12, as the protein in part A is slightly smaller and migrates further on the gel than in parts B and C.

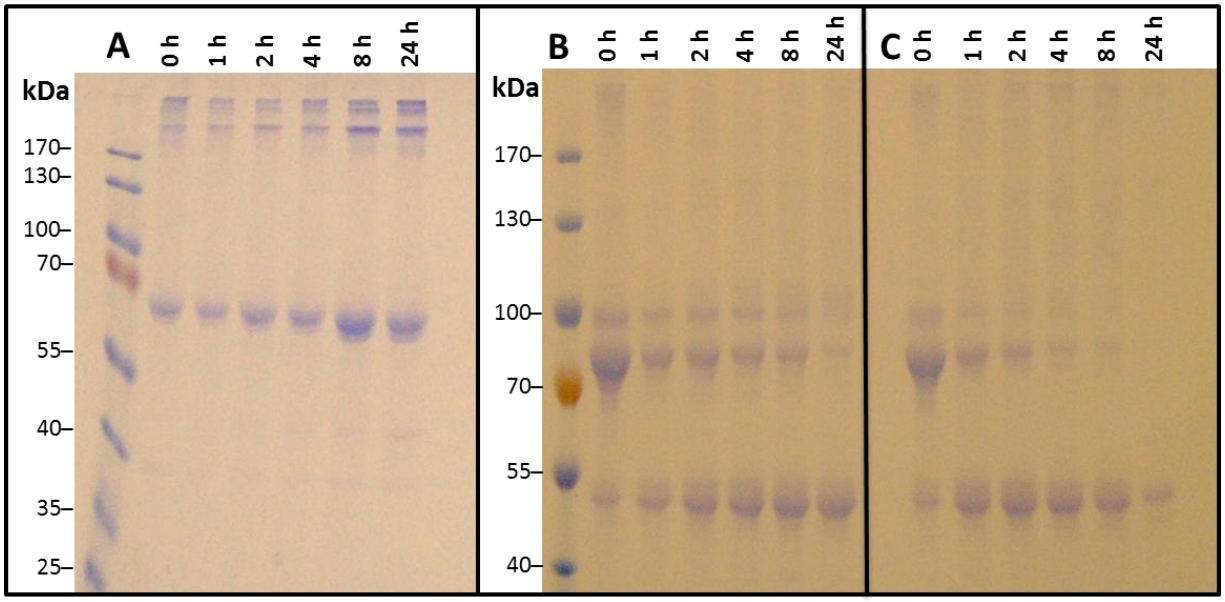

Figure 3.12. Optimisation of the thrombin cleavage assay.

A. GST-tagged Ire1 was incubated with 10 µl of thrombin beads and 20 µl samples were taken for analysis over the 24 h time course. A: At 4 °C, B: At 20 °C, C: At 37 °C. The Ire1 construct used in part A (truncated linker domain) was different from the one used in parts B and C (full length linker domain) as indicated in Figure 3.2.

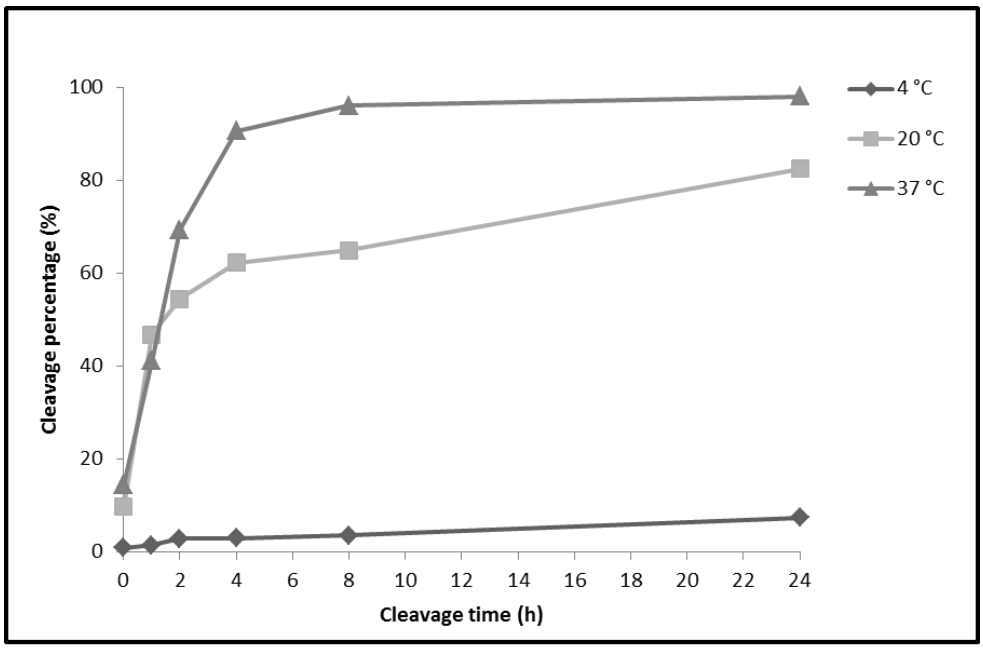

Figure 3.13. Quantification of the cleavage activity over time.

The bands from Figure 3.12 were quantified using ImageJ and the percentage of cleaved protein was plotted against time.

3.4.2 Thrombin cleavage has no effect on the protein kinase activity

To test if proteins retain kinase activity after removal of the GST tag, WT-Ire1 was incubated with thrombin over 24 h. Samples were taken at different time points and kinase assay was done. Figure 3.14 shows that [γ-^{32}P]ATP is still incorporated into the protein after 24 h and both GST-Ire1 and Ire1 have kinase activities. Quantification was done in the same way as for the previous protein kinase assay. The phosphoimager band intensity was divided by the Coomassie staining intensity and converted into percentage. Assuming that at the start of the experiment (0 h) the protein was 100% active, after 8 h and 24 h of incubation it retained ~95% and ~65% (Table 11) activity respectively. Again, the assay has its limitations in terms of quantification, but it shows that the protein retains its function, which is essentially the aim. All three tryptophan mutants also retain kinase activity after 24 h of thrombin cleavage (data not shown).

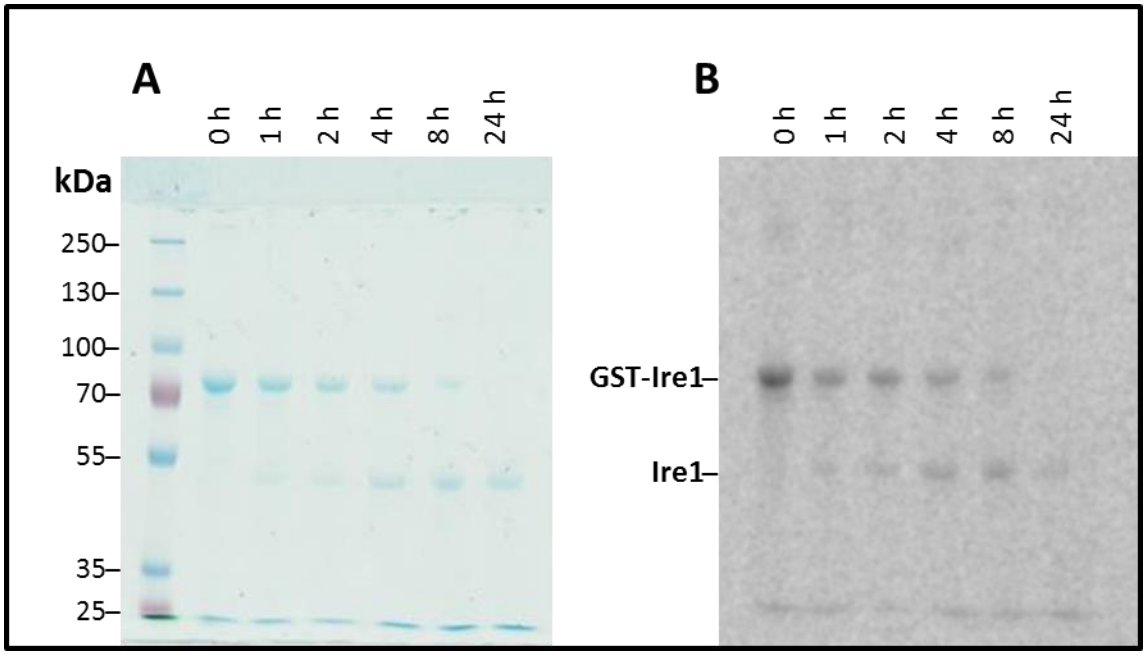

Figure 3.14. Thrombin cleaved WT-Ire1 retains kinase activity.
Kinase assay on thrombin cleaved samples over 24 h time course.
A. Coomassie brilliant blue staining
B. ^{32}P radioisotope detection using Typhoon 9400 variable mode imager

Table 11. Quantification of the protein kinase activity over 24 h.

Time	0 h	1 h	2 h	4 h	8 h	24 h
Activity (%)	100	74	109	80	95	64

3.4.3 Thrombin cleavage decreases the RNase activity over time

The next step after assessing the kinase activity was to test if removal of the GST-tag would affect the protein RNase activity. WT-Ire1 was incubated with thrombin beads and samples taken over the 24 h time course were tested for RNase activity. Figure 3.15 shows that the strong activity the wild type protein has at time zero is visibly reduced after 1 h. After 24 h the protein shows almost no activity suggesting that either long exposure to 20 °C or removal of the GST tag may inhibit the protein function or at least inhibit the dimerisation, which is needed for RNase activity (Zhou et al., 2006). Previous studies show that the activities of GST-fusion must be interpreted carefully due to the intrinsic property of GST to form dimers in solution (Niedziela-Majka et al., 1998). The result obtained here indicated that it may not be possible to prepare the tryptophan mutants for spectroscopic measurements, at least not in the time that was available to complete this project. However, since the RNA cleavage assay was optimised and there was an excess of the RNA substrate, some other mutants were purified and tested for activity, which will be described in the following chapter.

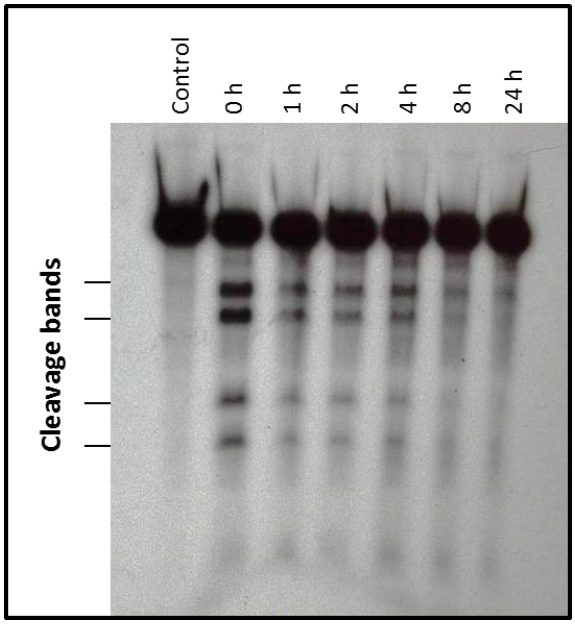

Figure 3.15. Thrombin cleavage results in decreased RNase activity over time.
RNA cleavage assay on WT-Ire1 incubated with thrombin for desired amount of time. Control lane contains RNA substrate only, other lanes contain the RNA substrate, ADP and WT-Ire1 incubated with thrombin for the indicated amount of time.

3.4.4 Separating the full length W855F-W981F-Ire1 from the truncated version

In order to still proceed towards large scale purifications, the one mutant retaining both protein kinase and RNase activities was used. Since it purifies as two bands, we attempted to separate the full length W855F-W981F-Ire1 from its truncated version. In theory, if the protein is truncated at the C-terminus by ~10 kDa, the theoretical pI of the proteins may be different enough to separate them using anion exchange chromatography. Ion exchange chromatography is based on the interaction between the resin and the proteins of opposite charges. At a pH equal to the isoelectric point (pI) of the protein, it will have no net charge. All proteins with lower pI than the buffer used will have negative charge and all proteins with higher pI than the buffer will have positive charge. In anion exchange chromatography, positively charged resin binds negatively charged proteins. Proteins bound to the matrix can be reversibly replaced by ions in solution, therefore, salt gradient allows eluting proteins at different salt concentrations. All the theoretical pI values for this experiment were calculated using the online ExPASy Server (Compute pI/Mw tool) (Bjellqvist et al., 1994; Gasteiger et al., 2005). The theoretical pI of the full length protein is 6.47. ~10 kDa smaller protein truncated at the C-terminus has a theoretical pI of 6.49, which is not different enough for separation. However, the theoretical pI difference of thrombin cleaved proteins may be big enough for dividing them (6.68 and 7.43 respectively). W855F-W981F-Ire1 was digested with thrombin for 24 h and loaded onto an anion exchange column. Two clear peaks were observed when eluting with 200 mM NaCl and 400 mM NaCl (Figure 3.16). SDS-PAGE analysis of the collected fractions showed some level of separation, but the results were inconclusive (data not shown). Eventually, due to lack of time and the observation that thrombin cleavage may negatively affect the RNase activity (see previous paragraph), the attempts to separate the proteins were abandoned.

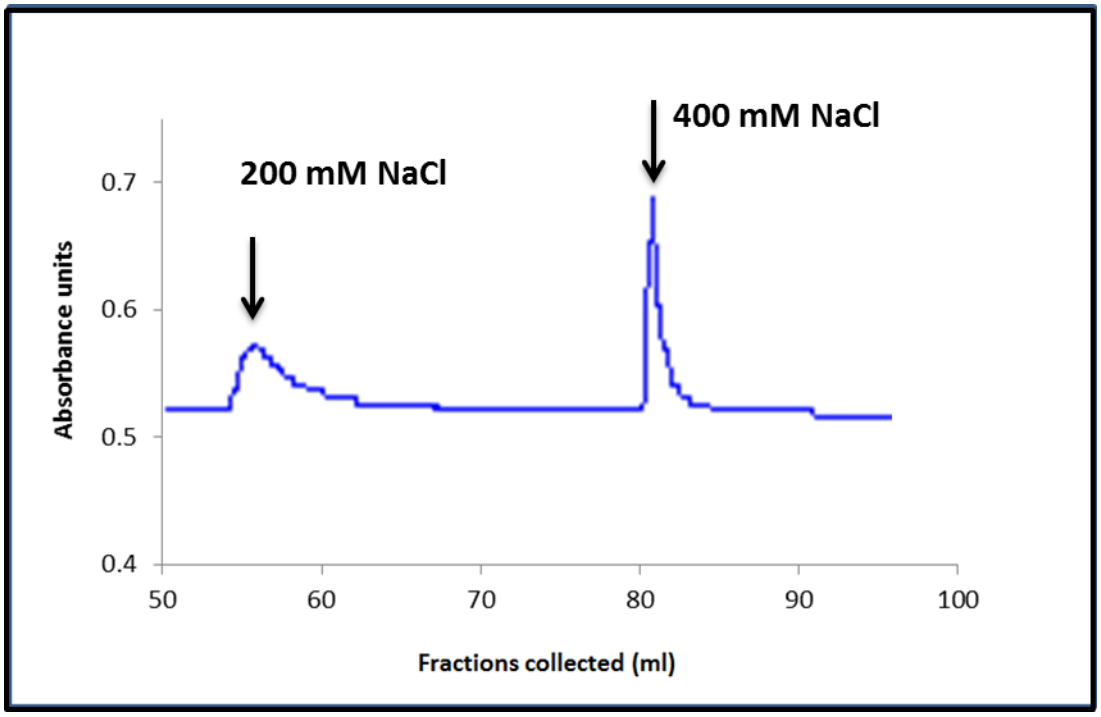

Figure 3.16. Anion exchange elution peaks for W855F-W981F-Ire1.
Proteins were eluted from anion exchange column with increasing salt concentration. Two clear peaks were observed when eluting with 200 mM NaCl and 400 mM NaCl as indicated above the graph.

3.4.5 Discussion

There are a number of modifications, which were not done due to lack of time, but could be done attempting to improve the purification of the tryptophan mutants. Temperature has been shown to have effects in protein folding (Baldwin, 1986), therefore, the induction conditions could be modified further to also test the effect of lower temperatures and different induction time. The protein could also be processed faster after the elution by using desalting columns instead of dialysis. Sonication conditions could be adjusted for more and shorter cycles to minimise heating up of the sample.

Overall, this chapter summarises the results of how thrombin cleavage affects the proteins used in this study. First of all, thrombin was shown to be inactive at 4 °C, which is the temperature preferred for all Ire1 manipulations. In order to avoid exposing the protein to 37 °C for extended period of time, 20 °C was selected as the optimal temperature for cleavage. However, it may be good to test the effect of shorter cleavage time at higher temperature, because the loss of activity could also be attributed to the extended time required for digest. As observed in Figure 3.13, 4 h at 37 °C is probably enough to cleave nearly all of the protein. This should be attempted in the future. Additionally, increased thrombin to Ire1 ratio in the assay may speed up the process and reduce the exposure time to higher temperatures.

The results also indicate that thrombin cleavage does not have a strong effect on the kinase activity, but it completely abolishes the RNase activity over time. Again, this may be attributed to temperature sensitivity or indicate that the dimer formation via the GST tags is essential for RNase activity. Previous studies showing that Ire1 on its own is capable to process mRNA also use GST-fusion proteins (Sidrauski and Walter, 1997). The protein may lose activity because it becomes a monomer. It would be interesting to repeat the experiments with increasing concentrations of Ire1, which may force Ire1 to dimerise again.

3.5 Characterisation of the RNase activity of the kinase mutants

3.5.1 K799A lacks kinase activity but retains RNase activity

As the RNA cleavage assay was finally working more reliably and an excess of RNA substrate was generated, some kinase mutants were also tested for RNase activity. For that, K799A-Ire1, N802A-Ire1, D828A-Ire1 and N802A-D828A-Ire1 were purified using affinity chromatography and dialysed as previously described.

All these have amino acid substitutions in the kinase domain and are fairly well characterised. K799 is a conserved catalytic residue in the nucleotide binding pocket predicted to coordinate the γ-phosphate of ATP (Rubio et al., 2011). N802 and D828 are Mg^{2+} coordinating residues. Again, the proteins were incubated with and without nucleotide to show that nucleotide binding is necessary for RNA cleavage activity. Figure 3.17 shows that apart from WT-Ire1, which was used as a positive control for the assay, only K799A-Ire1 shows some cleavage activity. Other mutations may potentially be involved in controlling conformational changes related Ire1 activation or to RNase activity.

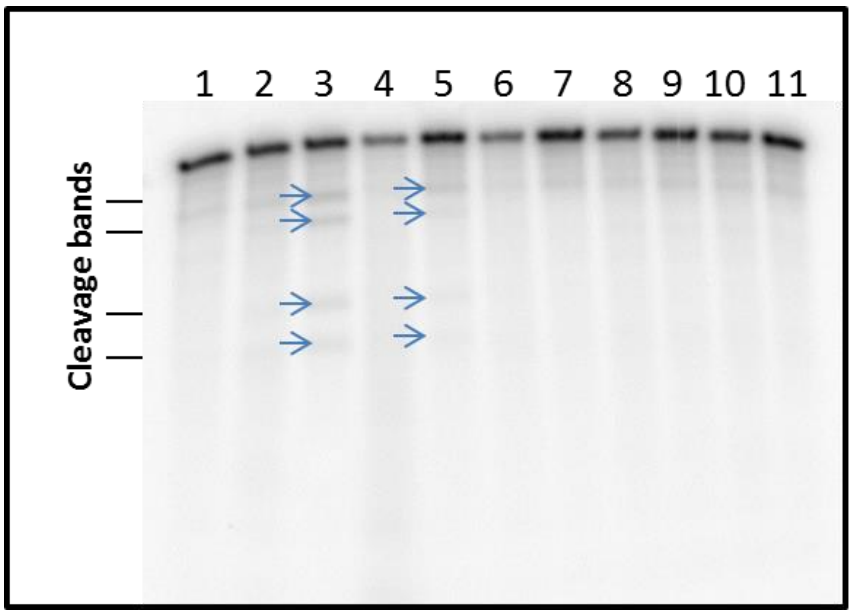

Figure 3.17. Only one kinase mutant shows RNase activity.
RNA cleavage assay on four kinase mutants indicates some activity of K799A-Ire1. WT-Ire1 was used as a positive control. The blue arrows show cleavage bands. Samples were loaded in the following order: RNA substrate only (Lane 1), RNA substrate + WT-Ire1 (lane 2), RNA substrate + WT-Ire1 + ADP (lane 3), RNA substrate + K799A-Ire1 (lane 4), RNA substrate + K799A-Ire1 + ADP (lane 5), RNA substrate + N802A-Ire1 (lane 6), RNA substrate +N802A-Ire1 + ADP (lane 7), RNA substrate + D828A-Ire1 (lane 8), RNA substrate + D828A-Ire1 + ADP (lane 9), RNA substrate + N802A-D828A-Ire1 (lane 10), RNA substrate + N802A-D828A-Ire1 + ADP (lane 11).

4 Final discussion

4.1 None of the tryptophan mutants retains all the features of WT-Ire1

As mentioned in the introduction, the intrinsic fluorescence of proteins owing to tryptophan is useful for studying the structure, dynamics and conformational changes. The principal fluorescence parameters of tryptophan such as the quantum yield, anisotropy, lifetimes, excitation and emission spectra are sensitive to the environment, therefore, this amino acid is used extensively as a probe for studying the protein structure (Lumry and Hershberger, 1978; Szabo and Rayner, 1980). The main aim of this study was to purify and characterise three single tryptophan mutants of yeast Ire1 in order to use them for such fluorescence measurements and better understand the ER stress sensor Ire1. Single tryptophan mutants of Ire1 have not been reported in the literature, however, the approach of producing Trp mutants generally has been known for a while (Markovic-Housley et al., 1999) . Protein structures are unique, so selecting the right amino acid substitution when generating mutants is very important. Tryptophan is usually substituted by phenylalanine or tyrosine due to their similar aromatic nature (Barnes and Gray, 2003). Phenylalanine and tryptophan both have very hydrophobic side chains and tyrosine is more reactive, therefore, phenylalanine was a reasonable choice for this study. Nevertheless, tryptophan is unique in size and its chemistry, so mutations can sometimes have negative effects. We decided to generate all three possible single tryptophan mutants for the cytosolic domain of yeast Ire1 and characterise them aiming to test all of them or alternatively pick the best one in terms of activity for fluorescence spectroscopy measurements.

4.1.1 Two out of three tryptophan mutants fail to purify as clean full-length proteins

Previously optimised methods were used to purify the cytosolic domain of yeast Ire1 and its mutants as GST-fusion proteins. The quality of WT-Ire1 and the kinase mutants purified using this protocol in the past encouraged us to assume that the tryptophan mutants could be easily purified in the same way and then be used for fluorescence analysis. However, the mutants did not always behave as expected. Only one of them (W855F-W1025F-Ire1) purified as a single full-length protein and the other two purified as a mixture of a full length and a truncated protein. Since the difference in protein size is so small (~10 kDa), we initially hypothesised that the second band on the gels may be attributed to different state of phosphorylation. As previously reported in the literature, the cytosolic domain of yeast Ire1 is phosphorylated when purified from *E. coli* as a GST-fusion protein (Sidrauski and Walter, 1997). Both the kinase autophosphorylation assay (Figure 3.9, Figure 3.10) and the λ protein phosphatase digest (Figure 3.5, Figure 3.6) show results consistent with previous reports. However, the tryptophan mutants used in this study are novel and no reports on their behaviour could be found. Hence, we hypothesised that the mutations may have disturbed the kinase activity partially and the two bands observed on the gels upon purification could show different states of phosphorylation. The λ protein phosphatase digest showed that both bands migrate further down after de-phosphorylation rejecting the hypothesis and suggesting the bottom band may be a truncated version of the protein. In that case, the protein must be shortened at the C-terminus, because the N-terminus has a GST tag and purification would not be possible without it.

4.1.2 All tryptophan mutants retain kinase activity but mutations in the RNase domain cause loss of endonuclease function

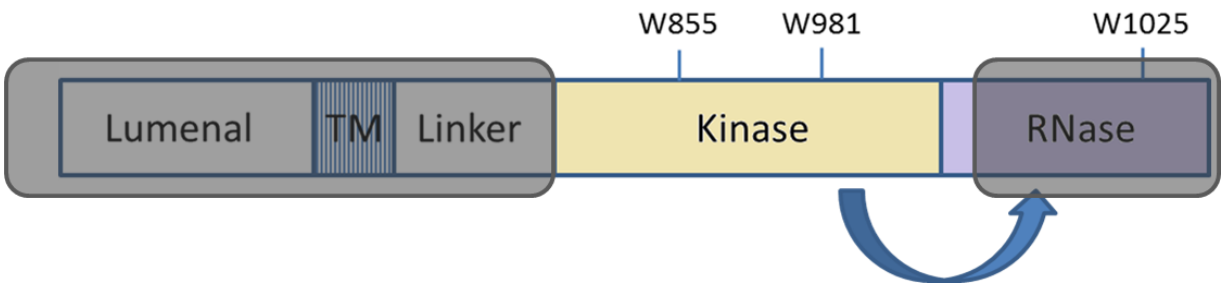

Figure 4.1. Simplified structure of Ire1.
A simplified diagram showing the structure of yeast Ire1. Tryptophan mutations are indicated above the graph. The arrow represents the idea that the kinase domain controls the RNase domain. The grey shaded portion on the left is the part of the protein, which was not used for purification and the grey shaded part on the right is the predicted missing portion of the truncated single tryptophan mutant.

This study shows that all the tryptophan mutants retain some kinase activity compared to WT-Ire1 (Figure 3.9, Figure 3.10). As for the RNase activity, the story is more complicated. Figure 4.1 shows a very simplified graphical representation of Ire1 with the mutated tryptophan residues indicated above. Two of these mutations are in the kinase domain and one in the RNase domain. Results show that the only mutant demonstrating some RNase activity is the mutant, which has both tryptophan substitutions in the kinase domain, suggesting that the W1025 residue must be essential for exerting the endonuclease function in Ire1.

Studies show that Ire1 RNase domain is activated in a unique manner (Korennykh et al., 2009) when the kinase domain is positioned for trans-autophosphorylation in a way that the RNase domain could bind the mRNA substrate. Oligomerisation is likely to generate additional mRNA binding surface and promote interactions not possible in lower oligomeric states of the protein. The domains and motifs of human RNase L and yeast Ire1 have some similarities (Figure 4.2) (Dong et al., 2001). The authors suggest that the human RNase L W632 is a homolog for yeast Ire1 W1025 residue. The study shows that mutating W632 to alanine inhibits RNase activity, but the effect of yeast W1025 mutation was not tested. Other homologous residues were also compared in this paper and the function is often different, however, it may indicate the direct involvement of W1025 in RNase activity. The authors also struggled to express

high levels of the W632A mutants in *E. coli*, suggesting the importance of this residue in correct protein folding.

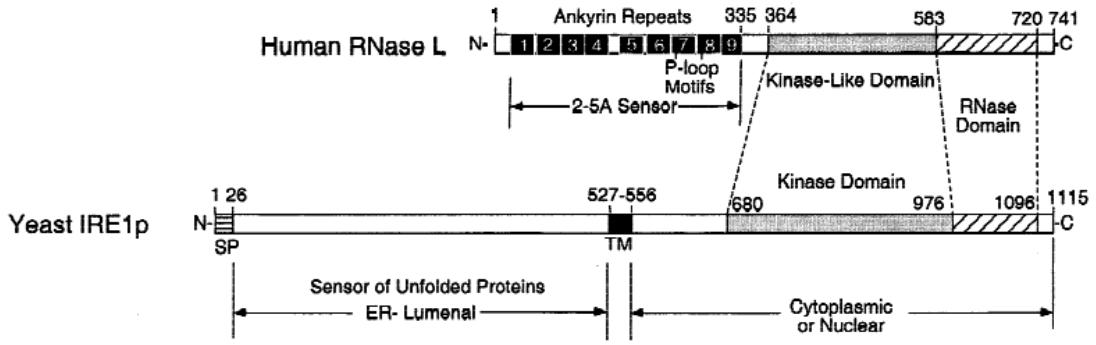

Figure 4.2. Comparison of the human RNase L and yeast Ire1 protein domains. SP:Signal peptide, TM: transmembrane domain.
Adapted from (Dong et al., 2001). Authors suggest that the two proteins have various homologous residues, including W632 of human RNase L and yeast Ire1 W1025.

The problem with the W855F-W981F-Ire1 mutant is that it contains a truncated version, which needs to be separated from the full-length protein. If the speculation that this mutant is truncated at the C-terminus is correct, it may have no RNase domain at all, because this is where the domain is located (see Figure 4.1). If nearly half of the protein used for activity assay is inactive, then the mutant protein is likely to be even more active than observed in this study.

Quantification of activity is another challenge faced during data analysis. Software such as ImageJ or ImageQuant designed for reporting intensities of gel bands was sensitive enough to detect them, however, in the context of control RNA substrate those bands were not much stronger than background. Quantified images always gave <5% cleavage for all the proteins. Thus, gel images rather than amount of cleavage in percentage was chosen as the way to present results.

4.1.3 Removal of the GST tag causes loss of function

One of the requirements for spectroscopy studies is to remove the GST tags from purified proteins because the GST has four tryptophan residues, which would interfere with the experiment and cause trouble interpreting the results. Thrombin cleavage assay was optimised in this study for small amounts of protein. Digests were carried out at 20 °C for 24 h (Figure 3.12, Figure 3.13). However, it was later discovered that this extended incubation time causes loss of RNase function. It is possible that exposure to 20 °C is the reason for function loss. It has been observed in the Schröder laboratory that Ire1 loses its activity over time when stored at -20 ºC and higher temperature is likely to speed up the process. However, as discussed before, cleavage at 37 °C for shorter time should be tested to see if the loss of activity may be attributed to prolonged exposure to higher temperature.

It has been reported that dimerisation is essential for Ire1 RNase function (Tirasophon et al., 2000) and mutations that inhibit dimerisation cause loss of UPR activation (Lee et al., 2008). Loss of activity over time in this case may be explained by slow removal of GST tags, whose crystal structures have been reported to have ability for dimer formation (Fabrini et al., 2009; Parker et al., 1990).

The crystal structure for human Ire1α has been determined and revealed that in the presence of ADP, the inactive Ire1 forms face-to-face dimers (Ali et al., 2011), different form the back-to-back dimers observed in RNase active conformation in yeast (Lee et al., 2008). Considering these observations, a potential mechanism of activation has been proposed recently (Walter and Ron, 2011). They suggest that in the presence of unfolded proteins, the lumenal domains rearrange to form front-to-front dimers, which correspond to pre-autophosphorylation complex. After autophosphorylation, the complex forms back-to-back dimers, which can then form higher order structures, which activate the RNase domain.

In the context of this study, it is possible that the low concentrations of monomeric Ire1 are unable to form higher order structures and, as a result, unable exert its RNA cleavage function.

The loss of RNase function was observed at the same time when separation of the two W855F-W981F-Ire1 proteins was attempted. The separation showed some progress and I strongly believe that the GST-free proteins can be separated using anion exchange chromatography. However, the observation that thrombin cleavage causes loss of activity led to stopping the experiments and briefly looking at the kinase mutants, because there was not enough time left to try and optimise the thrombin cleavage again. This would be one of the first things to do in the future studies to test the hypothesis that thrombin cleavage makes Ire1 monomeric and if larger amounts of protein may dimerise again. The purchased thrombin has the following activity: 200 µl of a 50% suspension of resin will cleave >85% of 1 mg of fusion protein in 1 ml in 4 hours at 20 °C (information provided in the RECOMT product technical bulletin). In order to optimise thrombin cleavage in less than 24 h, it would first be necessary to start purifying thrombin in the laboratory because it is much more cost effective. Commercially available thrombin is expensive, so purifying it in the lab would allow using larger amount of thrombin to reduce incubation time and possibly prevent activity loss. Potentially, thrombin may have reduced activity in the presence of the GST-elution buffer and the protein may need to be desalted into a different solution to increase activity. Alternatively, much larger concentrations of thrombin must be used to reduce the incubation time and preserve activity.

4.2 Ire1 Kinase activity is not essential for RNase activity

As described in the introduction, preliminary work in the lab suggested that K799, N802 and D828 are essential for controlling the RNase activity. K799 known for catalysing the γ phosphate transfer of ATP (Rubio et al., 2011), D828, known for coordinating the β and γ phosphates with Mg^{2+} (Chawla et al., 2011) and N802, which is also likely to be involved in coordinating Mg^{2+}. The proposed model suggests that ADP binding to the kinase domain activates the RNase domain of yeast Ire1 and therefore explains increased RNase activity of K799A, N802A and D828A mutants.

This study looks into the same mutants and provides contrasting results. Of course, the results are rather limited to draw conclusions, but lack of RNase activity was observed by N802A-Ire1, D828A-Ire1 and N802A-D828A-Ire1 (Figure 3.17). The only kinase mutant showing some RNase activity is K799A-Ire1 supporting the hypothesis

that phosphorylation may not be essential for XBP-1 splicing. It is not clear why other mutants have lost activity. The assay itself seemed to work well, both positive and negative controls worked as expected. The reasons may be similar to why the tryptophan mutants have lost activity, prolonged dialysis or overheating during the sonication when lysing the cells. The only certain conclusion drawn from the RNA cleavage assays is that nucleotide binding is always essential for RNase activity.

4.3 Future studies

If more time was available, it would be interesting to continue with this project using a variety of approaches.

Naturally, the first thing to do would be to try to further optimise the expression conditions for the tryptophan mutants, test lower temperatures and see if that affects protein folding. Adjusting the cell lysis conditions may also be useful. Performing all the manipulations at 4 °C and reducing the length of sonication cycles to prevent the protein from overheating may solve loss of activity issues.

In order to determine the nature of the truncated species, it would be interesting to elute the different bands from the SDS-PAGE gels and analyse them using mass spectrometry.

During the protein elution step, I would analyse a small amount of each fraction on a gel to see if all of them have truncated protein. If possible, I would only pool the fractions containing full length protein. If not, then I would try to change the *E. coli* expression system.

Alternatively, it would be interesting to try different substitutions of tryptophans to see if maybe the phenylalanines negatively affect the Ire1 function.

Optimising the thrombin cleavage again is necessary in order to test, whether larger amounts of Ire1 sustain RNase activity after removal of the GST tag. As mentioned before, low protein concentrations may favour the monomer, which causes the inactivity (Li et al., 2010).

Yeast survival assays for all the tryptophan mutants may also offer better understanding of the effect of these particular mutations on the protein activity. The yeast system offers some advantages like short growth time and easy genetic manipulations for various genetics and molecular biology experiments.

Another alternative would be to switch to more complex eukaryotic systems. Genetically manipulating human or mice cells to generate tryptophan mutants may allow doing a western blotting analysis using anti XBP-1 antibodies and testing if these particular mutations also reduce RNase activity in higher eukaryotes.

5 Conclusions

In conclusion, this study provides evidence that none of the single tryptophan mutants of yeast Ire1 can easily be used for fluorescence spectroscopy studies. W855F-W1025F-Ire1 purifies as a single full length protein, has kinase activity but lacks detectable RNA cleavage activity due to a tryptophan mutation in the RNase domain. W981F-W1025F-Ire1 purifies as two bands, a full length and possibly a truncated version. Most of this protein is truncated, it retains the kinase activity but also lacks RNase activity, again, most likely due to a mutation in the domain and because most of this protein purifies as a truncated version. W855F-W981F-Ire1 is the only mutant retaining kinase activity and showing some splicing potential, but it also purifies as two bands and a significant proportion of the protein used in the experiments was possibly truncated.

In order to still try and use W855F-W981F-Ire1, thrombin cleavage protocol to remove the GST tag must be optimised for much shorter time and/or lower temperature. In the case that these mutants retain activity after GST release, proteins may be separated using anion exchange chromatography. In the case this still results in lack of splicing, alternative mutations may be made. Tryptophan could also be mutated to alanine or other hydrophobic amino acids.

During this study, the RNA splicing assay was optimised from solving issues of reliably synthesising the RNA substrate *in vitro* to obtaining clear bands in the cleavage assay. This assay was used to show that GST release from the protein results in loss of RNase activity and that out of four kinase mutants tested here, only K799A-Ire1 has RNase activity. This result indicates that phosphotransfer may not be essential for XBP-1 splicing.

6 Bibliography

Ali, M.M.U., Bagratuni, T., Davenport, E.L., Nowak, P.R., Silva-Santisteban, M.C., Hardcastle, A., McAndrews, C., Rowlands, M.G., Morgan, G.J., Aherne, W., et al. (2011). Structure of the Ire1 autophosphorylation complex and implications for the unfolded protein response. EMBO J. *30*, 894–905.

Altmann, M., Edery, I., Trachsel, H., and Sonenberg, N. (1988). Site-directed mutagenesis of the tryptophan residues in yeast eukaryotic initiation factor 4E. Effects on cap binding activity. J. Biol. Chem. *263*, 17229–17232.

Baldwin, R.L. (1986). Temperature dependence of the hydrophobic interaction in protein folding. Proc. Natl. Acad. Sci. U. S. A. *83*, 8069–8072.

Barnes, M.R., and Gray, I.C. (2003). Bioinformatics for Geneticists (John Wiley & Sons).

Beechem, and Brand, and L. (1985). Time-Resolved Fluorescence of Proteins. Annu. Rev. Biochem. *54*, 43–71.

Bertolotti, A., Zhang, Y., Hendershot, L.M., Harding, H.P., and Ron, D. (2000). Dynamic interaction of BiP and ER stress transducers in the unfolded-protein response. Nat. Cell Biol. *2*, 326–332.

Bertolotti, A., Wang, X., Novoa, I., Jungreis, R., Schlessinger, K., Cho, J.H., West, A.B., and Ron, D. (2001). Increased sensitivity to dextran sodium sulfate colitis in IRE1beta-deficient mice. J. Clin. Invest. *107*, 585–593.

Bjellqvist, B., Basse, B., Olsen, E., and Celis, J.E. (1994). Reference points for comparisons of two-dimensional maps of proteins from different human cell types defined in a pH scale where isoelectric points correlate with polypeptide compositions. Electrophoresis *15*, 529–539.

Calfon, M., Zeng, H., Urano, F., Till, J.H., Hubbard, S.R., Harding, H.P., Clark, S.G., and Ron, D. (2002). IRE1 couples endoplasmic reticulum load to secretory capacity by processing the XBP-1 mRNA. Nature *415*, 92–96.

Cao, S.S., and Kaufman, R.J. (2012). Unfolded protein response. Curr. Biol. *22*, R622–R626.

Chawla, A., Chakrabarti, S., Ghosh, G., and Niwa, M. (2011). Attenuation of yeast UPR is essential for survival and is mediated by IRE1 kinase. J. Cell Biol. *193*, 41–50.

Clarke, H.J., Chambers, J.E., Liniker, E., and Marciniak, S.J. (2014). Endoplasmic Reticulum Stress in Malignancy. Cancer Cell *25*, 563–573.

Crowe, J.S., Cooper, H.J., Smith, M.A., Sims, M.J., Parker, D., and Gewert, D. (1991). Improved cloning efficiency of polymerase chain reaction (PCR) products after proteinase K digestion. Nucleic Acids Res. *19*, 184.

Dong, B., Niwa, M., Walter, P., and Silverman, R.H. (2001). Basis for regulated RNA cleavage by functional analysis of RNase L and Ire1p. RNA *7*, 361–373.

Eftink, M.R. (1991). Fluorescence Techniques for Studying Protein Structure. In Methods of Biochemical Analysis, C.H. Suelter, ed. (John Wiley & Sons, Inc.), pp. 127–205.

Endicott, J.A., Noble, M.E.M., and Johnson, L.N. (2012). The Structural Basis for Control of Eukaryotic Protein Kinases. Annu. Rev. Biochem. *81*, 587–613.

Fabrini, R., De Luca, A., Stella, L., Mei, G., Orioni, B., Ciccone, S., Federici, G., Lo Bello, M., and Ricci, G. (2009). Monomer-dimer equilibrium in glutathione transferases: a critical re-examination. Biochemistry (Mosc.) *48*, 10473–10482.

Fling, S.P., and Gregerson, D.S. (1986). Peptide and protein molecular weight determination by electrophoresis using a high-molarity tris buffer system without urea. Anal. Biochem. *155*, 83–88.

Fribley, A., Zhang, K., and Kaufman, R.J. (2009). Regulation of apoptosis by the unfolded protein response. Methods Mol. Biol. Clifton NJ *559*, 191–204.

Gasteiger, E., Hoogland, C., Gattiker, A., Duvaud, S. 'everine, Wilkins, M.R., Appel, R.D., and Bairoch, A. (2005). Protein Identification and Analysis Tools on the ExPASy Server. In The Proteomics Protocols Handbook, J.M. Walker, ed. (Humana Press), pp. 571–607.

Goldberg, J., Nairn, A.C., and Kuriyan, J. (1996). Structural basis for the autoinhibition of calcium/calmodulin-dependent protein kinase I. Cell *84*, 875–887.

Gonzalez, T.N., and Walter, P. (2001). Ire1p: a kinase and site-specific endoribonuclease. Methods Mol. Biol. Clifton NJ *160*, 25–36.

Green, R., and Rogers, E.J. (2013). Chemical Transformation of E. coli. Methods Enzymol. *529*, 329–336.

Hendershot, L.M., Ting, J., and Lee, A.S. (1988). Identity of the immunoglobulin heavy-chain-binding protein with the 78,000-dalton glucose-regulated protein and the role of posttranslational modifications in its binding function. Mol. Cell. Biol. *8*, 4250–4256.

Hubbard, S.R., Wei, L., and Hendrickson, W.A. (1994). Crystal structure of the tyrosine kinase domain of the human insulin receptor. Nature *372*, 746–754.

Imagawa, Y., Hosoda, A., Sasaka, S.-I., Tsuru, A., and Kohno, K. (2008). RNase domains determine the functional difference between IRE1alpha and IRE1beta. FEBS Lett. *582*, 656–660.

Janson, J.-C. (2012). Protein Purification: Principles, High Resolution Methods, and Applications (John Wiley & Sons).

Joshi, A., Newbatt, Y., McAndrew, P.C., Stubbs, M., Burke, R., Richards, M.W., Bhatia, C., Caldwell, J.J., McHardy, T., Collins, I., et al. (2015). Molecular mechanisms of human IRE1 activation through dimerization and ligand binding. Oncotarget *6*, 13019–13035.

Kimata, Y., Oikawa, D., Shimizu, Y., Ishiwata-Kimata, Y., and Kohno, K. (2004). A role for BiP as an adjustor for the endoplasmic reticulum stress-sensing protein Ire1. J. Cell Biol. *167*, 445–456.

Knighton, D.R., Zheng, J.H., Ten Eyck, L.F., Ashford, V.A., Xuong, N.H., Taylor, S.S., and Sowadski, J.M. (1991). Crystal structure of the catalytic subunit of cyclic adenosine monophosphate-dependent protein kinase. Science *253*, 407–414.

Korennykh, A.V., Egea, P.F., Korostelev, A.A., Finer-Moore, J., Zhang, C., Shokat, K.M., Stroud, R.M., and Walter, P. (2009). The unfolded protein response signals through high-order assembly of Ire1. Nature *457*, 687-U2.

Kosmaczewski, S.G., Edwards, T.J., Han, S.M., Eckwahl, M.J., Meyer, B.I., Peach, S., Hesselberth, J.R., Wolin, S.L., and Hammarlund, M. (2014). The RtcB RNA ligase is an essential component of the metazoan unfolded protein response. EMBO Rep. *15*, 1278–1285.

Kozutsumi, Y., Segal, M., Normington, K., Gething, M.-J., and Sambrook, J. (1988). The presence of malfolded proteins in the endoplasmic reticulum signals the induction of glucose-regulated proteins. Nature *332*, 462–464.

Lee, A.S. (1992). Mammalian stress response: induction of the glucose-regulated protein family. Curr. Opin. Cell Biol. *4*, 267–273.

Lee, A.S. (2005). The ER chaperone and signaling regulator GRP78/BiP as a monitor of endoplasmic reticulum stress. Methods *35*, 373–381.

Lee, K.P.K., Dey, M., Neculai, D., Cao, C., Dever, T.E., and Sicheri, F. (2008). Structure of the Dual Enzyme Ire1 Reveals the Basis for Catalysis and Regulation in Nonconventional RNA Splicing. Cell *132*, 89–100.

Li, H., Korennykh, A.V., Behrman, S.L., and Walter, P. (2010). Mammalian endoplasmic reticulum stress sensor IRE1 signals by dynamic clustering. Proc. Natl. Acad. Sci. U. S. A. *107*, 16113–16118.

Lindberg, R.A., Quinn, A.M., and Hunter, T. (1992). Dual-specificity protein kinases: will any hydroxyl do? Trends Biochem. Sci. *17*, 114–119.

Liu, C.Y., Wong, H.N., Schauerte, J.A., and Kaufman, R.J. (2002). The protein kinase/endoribonuclease IRE1alpha that signals the unfolded protein response has a luminal N-terminal ligand-independent dimerization domain. J. Biol. Chem. *277*, 18346–18356.

Lu, Y., Liang, F.-X., and Wang, X. (2014). A Synthetic Biology Approach Identifies the Mammalian UPR RNA Ligase RtcB. Mol. Cell *55*, 758–770.

Lumry, R., and Hershberger, M. (1978). Status of Indole Photochemistry with Special Reference to Biological Applications. Photochem. Photobiol. *27*, 819–840.

Markovic-Housley, Z., Stolz, B., Lanz, R., and Erni, B. (1999). Effects of tryptophan to phenylalanine substitutions on the structure, stability, and enzyme activity of the IIAB(Man) subunit of the mannose transporter of Escherichia coli. Protein Sci. *8*, 1530–1535.

Mogi, T., Marti, T., and Khorana, H.G. (1989). Structure-function studies on bacteriorhodopsin. IX. Substitutions of tryptophan residues affect protein-retinal interactions in bacteriorhodopsin. J. Biol. Chem. *264*, 14197–14201.

Möller, M., and Denicola, A. (2002). Protein tryptophan accessibility studied by fluorescence quenching. Biochem. Mol. Biol. Educ. *30*, 175–178.

Mori, K. (2009). Signalling Pathways in the Unfolded Protein Response: Development from Yeast to Mammals. J. Biochem. (Tokyo) *146*, 743–750.

Mori, K., Ma, W., Gething, M.-J., and Sambrook, J. (1993). A transmembrane protein with a cdc2+CDC28-related kinase activity is required for signaling from the ER to the nucleus. Cell *74*, 743–756.

Munro, S., and Pelham, H.R. (1986). An Hsp70-like protein in the ER: identity with the 78 kd glucose-regulated protein and immunoglobulin heavy chain binding protein. Cell *46*, 291–300.

Nekrutenko, A., and He, J. (2006). Functionality of unspliced XBP1 is required to explain evolution of overlapping reading frames. Trends Genet. *22*, 645–648.

Niedziela-Majka, A., Rymarczyk, G., Kochman, M., and Ożyhar, A. (1998). GST-Induced Dimerization of DNA-Binding Domains Alters Characteristics of Their Interaction with DNA. Protein Expr. Purif. *14*, 208–220.

Nolen, B., Taylor, S., and Ghosh, G. (2004). Regulation of Protein Kinases: Controlling Activity through Activation Segment Conformation. Mol. Cell *15*, 661–675.

Özcan, U., Cao, Q., Yilmaz, E., Lee, A.-H., Iwakoshi, N.N., Özdelen, E., Tuncman, G., Görgün, C., Glimcher, L.H., and Hotamisligil, G.S. (2004). Endoplasmic Reticulum Stress Links Obesity, Insulin Action, and Type 2 Diabetes. Science *306*, 457–461.

Papa, F.R., Zhang, C., Shokat, K., and Walter, P. (2003). Bypassing a Kinase Activity with an ATP-Competitive Drug. Science *302*, 1533–1537.

Parker, M.W., Bello, M.L., and Federici, G. (1990). Crystallization of glutathione S-transferase from human placenta. J. Mol. Biol. *213*, 221–222.

Repaske, R. (1958). Lysis of gram-negative organisms and the role of versene. Biochim. Biophys. Acta *30*, 225–232.

Rinaldi, A.J., Suddala, K.C., and Walter, N.G. (2015). Native purification and labeling of RNA for single molecule fluorescence studies. Methods Mol. Biol. Clifton NJ *1240*, 63–95.

Rubio, C., Pincus, D., Korennykh, A., Schuck, S., El-Samad, H., and Walter, P. (2011). Homeostatic adaptation to endoplasmic reticulum stress depends on Ire1 kinase activity. J. Cell Biol. *193*, 171–184.

Sambrook, J., and Russel, D.W. (2001). Molecular Cloning: A Laboratory Manual (Cold Spring Harbor, New York: Cold Spring Harbor Laboratory Press).

Shamu, C.E., and Walter, P. (1996). Oligomerization and phosphorylation of the Ire1p kinase during intracellular signaling from the endoplasmic reticulum to the nucleus. EMBO J. *15*, 3028–3039.

Shiu, R.P., Pouyssegur, J., and Pastan, I. (1977). Glucose depletion accounts for the induction of two transformation-sensitive membrane proteinsin Rous sarcoma virus-transformed chick embryo fibroblasts. Proc. Natl. Acad. Sci. U. S. A. *74*, 3840–3844.

Sicheri, F., and Silverman, R.H. (2011). Putting the brakes on the unfolded protein response. J. Cell Biol. *193*, 17–19.

Sidrauski, C., and Walter, P. (1997). The transmembrane kinase Ire1p is a site-specific endonuclease that initiates mRNA splicing in the unfolded protein response. Cell *90*, 1031–1039.

Sidrauski, C., Cox, J.S., and Walter, P. (1996). tRNA Ligase Is Required for Regulated mRNA Splicing in the Unfolded Protein Response. Cell *87*, 405–413.

Studier, F.W. (2005). Protein production by auto-induction in high-density shaking cultures. Protein Expr. Purif. *41*, 207–234.

Szabo, A.G., and Rayner, D.M. (1980). Fluorescence decay of tryptophan conformers in aqueous solution. J. Am. Chem. Soc. *102*, 554–563.

Tirasophon, W., Lee, K., Callaghan, B., Welihinda, A., and Kaufman, R.J. (2000). The endoribonuclease activity of mammalian IRE1 autoregulates its mRNA and is required for the unfolded protein response. Genes Dev. *14*, 2725–2736.

Todd, D.J., Lee, A.-H., and Glimcher, L.H. (2008). The endoplasmic reticulum stress response in immunity and autoimmunity. Nat. Rev. Immunol. *8*, 663–674.

Valkonen, M., Penttilä, M., and Saloheimo, M. (2004). The ire1 and ptc2 genes involved in the unfolded protein response pathway in the filamentous fungus Trichoderma reesei. Mol. Genet. Genomics *272*, 443–451.

Walter, P., and Ron, D. (2011). The unfolded protein response: from stress pathway to homeostatic regulation. Science *334*, 1081–1086.

Wang, Z.-X., and Wu, J.-W. (2002). Autophosphorylation kinetics of protein kinases. Biochem. J. *368*, 947–952.

Welihinda, A.A., and Kaufman, R.J. (1996). The unfolded protein response pathway in Saccharomyces cerevisiae. Oligomerization and trans-phosphorylation of Ire1p (Ern1p) are required for kinase activation. J. Biol. Chem. *271*, 18181–18187.

Witholt, B., and Boekhout, M. (1978). The effect of osmotic shock on the accessibility of the murein layer of exponentially growing Escherichia coli to lysozyme. Biochim. Biophys. Acta BBA - Biomembr. *508*, 296–305.

Ye, J., Rawson, R.B., Komuro, R., Chen, X., Davé, U.P., Prywes, R., Brown, M.S., and Goldstein, J.L. (2000). ER Stress Induces Cleavage of Membrane-Bound ATF6 by the Same Proteases that Process SREBPs. Mol. Cell *6*, 1355–1364.

Yoshida, H., Matsui, T., Yamamoto, A., Okada, T., and Mori, K. (2001). XBP1 mRNA Is Induced by ATF6 and Spliced by IRE1 in Response to ER Stress to Produce a Highly Active Transcription Factor. Cell *107*, 881–891.

Zhang, F., Strand, A., Robbins, D., Cobb, M.H., and Goldsmith, E.J. (1994). Atomic structure of the MAP kinase ERK2 at 2.3 Å resolution. Nature *367*, 704–711.

Zhou, J., Liu, C.Y., Back, S.H., Clark, R.L., Peisach, D., Xu, Z., and Kaufman, R.J. (2006). The crystal structure of human IRE1 luminal domain reveals a conserved dimerization interface required for activation of the unfolded protein response. Proc. Natl. Acad. Sci. U. S. A. *103*, 14343–14348.